

Microwave-induced resistance oscillations in highly viscous electron fluid

P. S. Alekseev and A. P. Alekseeva
Ioffe Institute, 194021 St. Petersburg, Russia

Hydrodynamics of conduction electrons has been recently discovered in graphene [1–6], ultra-pure metals [7, 8], and high-mobility GaAs quantum wells [9–14]. Here we demonstrate that the microwave-induced resistance oscillations (MIRO) observed in best-quality GaAs quantum wells [15, 16] can be explained within a hydrodynamic model and evidence about the formation of a highly viscous fluid, a previously unexplored phase of strongly correlated 2D electrons. We construct a model of the hydrodynamic magnetotransport in a strongly non-ideal 2D electron fluid at microwave radiation. The viscoelastic dynamics of the fluid and the memory effect in the interparticle scattering lead to magnetooscillations of photoresistance, similar to MIRO. In addition to the properties of MIRO explained by theories [17–22] for non-interacting 2D electrons, our theory predicts an irregular shape of the oscillations at certain sample sizes and no dependence of the oscillations on the sign of the circular polarization of radiation. The latter properties were observed in best-quality samples [15, 16], but remained mysterious until now. Based on this result and on explanation [23] of sharp anomalies in photoresistance of similar structures [24–26] by the excitation of transversal magnetosound, characteristic for the viscoelastic dynamics, we conclude that 2D electrons in some best-quality GaAs quantum wells form a highly viscous fluid.

1. Introduction. Microwave-induced resistance oscillations (MIRO) of 2D electrons in high-mobility conductors in moderate magnetic fields is an intriguing effect, whose correct explanation is, apparently, crucial for understanding of the nature of transport phenomena in such systems. MIRO was initially observed [27–29] and then extensively studied [30] on the high-mobility GaAs quantum wells, similar to the ones in which the fractional quantum Hall effect was discovered.

Originally, MIRO were attributed to transitions of non-interacting 2D electrons at high Landau levels in external dc and ac electric fields [17–20]. Such displacement mechanism [31, 32] is based on taking into account the radiation-assisted scattering of 2D electrons in quantized states on disorder, that result in unequal probabilities of electron transitions in the opposite directions at a dc field. Theories [17, 18] yield the correct profile of the magnetooscillations of photoresistance. In Refs. [19] the inelastic mechanism was proposed in which the crucial role is played by radiation-induced redistribution of elec-

trons by energy. Its contribution to photoresistance explains the temperature dependence of MIRO. In Ref. [21] it was shown that the classical memory effects in scattering of 2D electrons on disorder can lead to magnetooscillations in photoresistance similar to MIRO.

In Ref. [22] a different powerful approach to the theory of MIRO was developed. It is based on a phenomenological description of the memory effects in classical dynamics of non-interacting 2D electrons, being scattered on localized defects. Theory [22], supported by numerical experiments (their results are presented also in Ref. [22]), describes MIRO in a self-consistent and lucid way.

Theories [17–22] have a substantial problem which is the inconsistency between the lack of dependence of the effect on the sign of the circular polarization of radiation in some experiments [15, 16] and the presence of this dependence in theory [33–36]. In addition, in best-quality GaAs quantum wells were observed [15, 16, 24, 25] strange features in MIRO (a non-sinusoidal profile, a giant peak), unexplained within disorder-based theories.

In parallel with the studies of MIRO, the giant negative magnetoresistance was observed in the same high-mobility GaAs quantum wells [9–12, 14, 24]. In Ref. [13] it was explained as the result of formation of a viscous fluid from 2D electrons in the quantum wells [37]. Later, a very similar huge negative magnetoresistance was detected also in other high-quality conductors: 2D metal PdCoO₂ [7], the 3D Weyl semimetal WP₂ [8], and single-layer graphene [4, 5]. For those conductors, other strong evidences of realization of the hydrodynamic electron transport were previously discovered [1–3, 6].

Beside this, resonant properties of the 2D electron viscous fluid were revealed. It was shown that the high-frequency viscosity coefficients of 2D electrons exhibit the magnetic resonance related to the perturbations of the shear stress [38]. In strongly non-ideal electron Fermi fluids such resonance manifests itself via the transverse magnetosonic waves [23]. We argued [23] that this effect is responsible for the peak and other anomalies observed in photoresistance and photovoltage at the doubled cyclotron frequency in the best-quality structures [24–26].

In this way, it is reasonable to expect that a significant contribution to MIRO in highest-mobility GaAs quantum wells originates from the hydrodynamic component of the electron flow. Here we construct a theoretical model of ac magnetotransport in a strongly non-ideal (highly viscous) 2D electron fluid. For this type of fluids, the theory turns out to be simple and bright. Following to the approach of Ref. [22], we formulate phenomenological equations of dynamics of the fluid those are the Drude-like viscoelas-

tic equations of Ref. [23] supplemented by the retarded relaxation term accounting the classical memory effect in interparticle collisions. The calculated photoconductivity of a Poiseuille flow exhibits magnetooscillations, which are very similar to MIRO. In particular, they can have a sinusoidal or an irregular shape for different sample widths (in the linear by radiation power limit), and, for circularly polarized radiation, are independent of the sign of the polarization. Both these properties were observed for MIRO in the GaAs wells of highest mobilities [15, 16] (irregular oscillations were possibly observed also in Refs. [24, 25]). The obtained results, together with explanation [23] of the sharp anomalies in photoresistance of similar samples [24–26] within a viscoelastic model, signify that 2D electrons in some high-mobility GaAs quantum wells form a highly viscous fluid.

2. *Model.* At high frequencies, $\omega \gg 1/\tau_2$, the dynamics of a strongly non-ideal electron fluid resembles the one of an elastic media, in which the interparticle interaction mainly determines the elastic internal forces and the role of relaxation due to interparticle scattering is weak [23, 39, 40] (τ_2 is the shear stress relaxation time). A high-frequency flow of such electron media, similar to uncharged highly viscous fluids, is approximately described by the displacement of its small elements $\mathbf{u}(\mathbf{r}, t)$. In this near-elastic flow the “slipping” of neighbor layers is very weak, that corresponds to the direct connection between \mathbf{u} and the hydrodynamic velocity \mathbf{V} :

$$\partial \mathbf{u}(\mathbf{r}, t) / \partial t \approx \mathbf{V}(\mathbf{r}, t). \quad (1)$$

General dynamics of the viscous electron fluid, accounting the interparticle scattering and substantial slipping, is described by the density n , the velocity \mathbf{V} , and the non-equilibrium momentum flux tensor Π_{ij} , related to the shear stress tensor. Equation (1) in this case is a formula for calculation of the displacement $\mathbf{u}(\mathbf{r}, t)$ in the linear by \mathbf{V} approximation. The value \mathbf{u} alone in this case is not sufficient to describe the fluid dynamics.

A high-frequency flow of a highly viscous 2D electron fluid is formed by the plasmons related to perturbations of the electron density n and by the transversal waves related to perturbations of the shear stress $\hat{\Pi}$ [23]. The last ones are governed by the dissipativeless shear-stress part of interparticle interaction, described by the Landau interaction term within the Fermi-liquid model [23, 39]. The interparticle scattering leads to a weak relaxation of both the plasmonic \mathbf{V}_p and the viscoelastic \mathbf{V}_s flow components. The Navier-Stokes equation for a strongly non-ideal electron fluid were derived in Ref. [39] for zero magnetic field and in Ref. [40] for a nonzero magnetic field. Although only the case of a very strong interparticle interaction was considered in [40] for simplicity (large Landau parameters, $F_m \gg 1$), the motion equations obtained there seems to remain qualitatively valid also at a moderate interaction ($F_m \sim 1$). The near-elastic dynamic of the fluid, obeying Eq. (1), is realized when ω

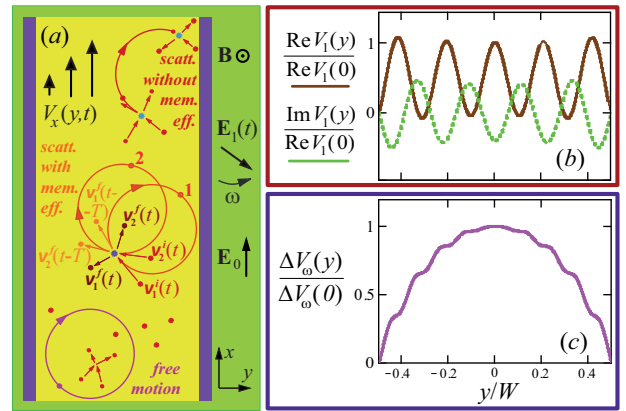


FIG. 1: (a) Flow of a highly viscous 2D electron fluid in a long defectless sample in a magnetic field \mathbf{B} , a dc electric field \mathbf{E}_0 , and a circularly polarized radiation field $\mathbf{E}_1(t)$. Trajectories of two Fermi liquid quasiparticles in an extended collision, leading to the memory effect, as well as trajectories of a collisionless motion and of two successive collisions without the memory effect are drawn. (b) Ac component $V_1(y) \sim E_1$ of the flow in a long sample with rough edges. (c) Radiation-induced correction $V_\omega(y)$ to the dc flow component $V_0(y) \sim E_0$ in the same sample. All curves are plotted for the parameters: $\omega\tau_2 = 40$, $\tau_q/\tau_2 = 0.7$, $W/L_s = 1$, and $\omega_c/\omega = 0.34$. The wavelength and the decay length of the magnetosonic waves are: $2\pi/\text{Im}\lambda = 0.21 W$ and $1/\text{Re}\lambda = 1.00 W$.

is far from the cyclotron and the viscoelastic resonances $\omega = \omega_c$, $2\omega_c$ [23] (here ω_c is the cyclotron frequency).

The memory effects in scattering of non-interacting 2D electrons on localized impurities in a perpendicular magnetic field \mathbf{B} [22, 43–45] originate from the possibility for electrons to experience no collisions or several returning to the same impurity (“extended collisions”), depending on the positions of trajectories relative to impurities.

For a strongly non-ideal 2D electron fluid in a magnetic field, a similar memory effect originates from successive collisions of electron-like quasiparticles, joined in pairs {see Fig. 1(a) and Supplemental information [47]}. Such “extended interparticle collisions” can be interrupted by a collision of a particle in a pair with a third particle. We account for these events in the fluid dynamic equation, extending the equations of [13, 23, 40], by adding the retarded interparticle relaxation term, similar to the retarded electron-disorder relaxation term in Ref. [22]:

$$\begin{aligned} \partial n / \partial t + n_0 \text{div} \mathbf{V} &= 0, \\ \partial(mV_i) / \partial t &= eE_i(\mathbf{r}, t) + m\omega_c \epsilon_{ikz} V_k - \partial \Pi_{ij} / \partial x_j, \\ \partial \Pi_{ij} / \partial t &= 2\omega_c \epsilon_{ikz} \Pi_{kj} - m(v_F^n)^2 V_{ij} / 4 - \\ &\quad - \Pi_{ij} / \tau_2 - \Gamma_{ijkl}(\mathbf{r}, t) \Pi_{kl}(\mathbf{r}, t - T). \end{aligned} \quad (2)$$

Here $n_0 = n - \delta n$ is the equilibrium density; the electric field \mathbf{E} consists of the applied field and the internal field

induced by a non-equilibrium charge density $e\delta n(\mathbf{r}, t)$: $\mathbf{E}(\mathbf{r}, t) = \mathbf{E}^{ext}(t) + \mathbf{E}^{int}(\mathbf{r}, t)$; e and m are the electron charge and the effective mass; ϵ_{ikm} is the antisymmetric unit tensor; $V_{ij} = \partial V_i/\partial x_j + \partial V_j/\partial x_i$; τ_2 is the shear stress relaxation time without the memory effects, calculated, for example, in Refs. [41, 42]; v_F^η is the parameter defining the magnitude of the viscosity η of a highly viscous fluid [23]: $\eta|_{B=0} = (v_F^\eta)^2 \tau_2/4$; and $T = 2\pi/\omega_c$ is the cyclotron period.

The term $-\Gamma_{ijkl}(\mathbf{r}, t)\Pi_{kl}(\mathbf{r}, t-T)$ in Eq. (2) describes the retarded relaxation of Π_{ij} due to the extended collisions of pairs of quasiparticles with one return to the same point [see Fig. 1(a)]. Extended collisions are sensitive to the macroscopic motion of the fluid via the forces acting on quasiparticles from the internal field \mathbf{E}^{int} and from the elastic tension. The latter one is induced by perturbations of the quasiparticle energy spectrum by nonzero \mathbf{V} and leads to the term $-m(v_F^\eta)^2 V_{ij}/4$ in Eq. (2) [39, 40]. Because of these sensitivity, the tensor $\hat{\Gamma}(\mathbf{r}, t)$ depends on the variables characterizing the fluid in the past, $t' < t$. For example, the probability to return to the same scattering configuration for two quasiparticles is much greater for a stationary homogeneous flow than for a fast ac flow with large-amplitude oscillations, in which the memory about positions of two quasiparticles is typically lost in a cyclotron rotation [see Fig. 1(a)].

At the near-elastic motion with weak interparticle scattering, the tensor $\hat{\Gamma}(\mathbf{r}, t)$ depends only on the shift of the strain tensor, $\epsilon_{mn} = \partial u_m/\partial x_n + \partial u_n/\partial x_m$, in one cyclotron period: $\Delta_{mn}(\mathbf{r}, t) = \epsilon_{mn}(\mathbf{r}, t) - \epsilon_{mn}(\mathbf{r}, t-T)$ (for details see [47]). For a small-amplitude oscillating flow, $\hat{\Gamma}(\mathbf{r}, t) = \hat{\Gamma}(\hat{\Delta}(\mathbf{r}, t))$ is expanded into power series by $\hat{\Delta}$:

$$\Gamma_{ijkl}(\hat{\Delta}) = \Gamma_{ijkl}^{(0)} + \alpha_{ijkl}^{mnop} \Delta_{mn} \Delta_{op}, \quad (3)$$

where $\Gamma_{ijkl}^{(0)}$ and α_{ijkl}^{mnop} are proportional to the probability $P = e^{-T/\tau_q}$ to make a full cyclotron rotation (here $\tau_q \lesssim \tau_2$ is the interparticle departure scattering time). Such description of the memory effect in rare interparticle collisions is applicable far from the viscoelastic and the cyclotron resonances $|\omega - \omega_c|$, $|\omega - 2\omega_c| \lesssim 1/\tau_2$, where the flow is determined by the interparticle already in the main approximation.

In this way, we formulated a closed system of nonlinear equations (1)-(3) describing the evolution of n , \mathbf{V} , and Π_{ij} in a highly viscous fluid in defectless samples. Note that the importance of the retarded term in Eq. (2) implies that the contribution from the deterministic dynamics, reflected by the extended collisions, is substantial for the formation of a flow.

3. Photoconductivity of Poiseuille flow. We consider a Poiseuille flow in a defectless long sample as a minimal model to the study the effect of radiation on dc magnetotransport in a highly viscous electron fluid [see Fig. 1(a)]. The external electric field $\mathbf{E}^{ext}(t) = \mathbf{E}_0 + \mathbf{E}_1(t)$ consist of the dc field $\mathbf{E}_0 = E_0 \mathbf{e}_x$ induced by

an applied electric bias and the radiation field $\mathbf{E}_1(t) = \mathbf{E}_1^\pm e^{-i\omega t} + c.c.$ with the left or the right circular polarizations: $\mathbf{E}_1^\pm = E_1(1/2, \pm i/2)$. The sample edges are supposed to be rough, thus the fully diffusive boundary conditions, $\mathbf{V}|_{y=\pm W/2} = 0$, are applicable. The internal field $\mathbf{E}^{int}(y, t)$ in this geometry is directed along the y axis, being the Hall field. The sample is considered to be narrow: $W \ll l_p$, where l_p is the characteristic plasmon wavelength. In such case, the field $\mathbf{E}^{int}(y, t)$ screens the y component of the incident ac field $\mathbf{E}_1(t)$; the ac plasmonic flow component \mathbf{V}_p , related to $\delta n(y, t)$, is suppressed; and the ac component of the flow is formed mainly by the viscoelastic eigenmodes: $\mathbf{V}_1 \approx \mathbf{V}_s$ [23, 47]. Herewith only the x component of the velocity $\mathbf{V} = \mathbf{V}_0 + \mathbf{V}_1$ and the xy component of the tensors V_{ij} and ϵ_{ij} presents in both the ac and the dc flow components.

To find photoconductivity, first, one needs the linear responses on the dc \mathbf{E}_0 and the ac $\mathbf{E}_1(t)$ electric fields. The response on the dc field is a 2D Poiseuille flow with a parabolic profile: $V_0(y) = eE_0[(W/2)^2 - y^2]/(2m\eta_{xx})$, depending on magnetic field via the dc diagonal viscosity η_{xx} [13]. The linear response on the ac fields of the both polarizations \mathbf{E}_1^\pm is expressed via the function $f_\lambda(y) = \cosh(\lambda y)/\cosh(\lambda W/2)$ as [23]: $V_1(y, t) = V_1(y) e^{-i\omega t} + c.c.$, where $V_1(y) = ieE_1[1 - f_\lambda(y)]/(2m\omega)$,

$$\lambda = \sqrt{-i\omega/\eta_{xx}(\omega)} \quad (4)$$

is the eigenvalue of the transverse magnetosonic waves, and $\eta_{xx}(\omega)$ is the ac diagonal viscosity. In the viscoelastic regime, $\omega \sim \omega_c \gg 1/\tau_2$, the imaginary parts dominate in $\eta_{xx}(\omega)$ far from the resonance $\omega = 2\omega_c$, therefore Eqs. (2) turns out into Hooke's equations and Eq. (1) becomes valid [40]. The wavelength and the decay length of the transverse waves at $\omega > 2\omega_c$ are estimated from Eq. (4) as $l_s = v_F^\eta/\omega$ and $L_s = v_F^\eta \tau_2$ [47]. The parameter v_F^η in a highly viscous fluid is much greater than the Fermi velocity v_F , thus a flow with characteristic spacescales $l_s \gg v_F/\omega$ can be described hydrodynamically [23, 40].

Second, to calculate the small photoconductivity proportional the radiation power $\mathcal{W} \sim E_1^2$ we need the following contributions in the hydrodynamic velocity: $V = V_0 + V_1 + V_\omega$, where V_0 and V_1 are the dc and ac linear responses presented above and $V_\omega = V_\omega(y)$ is the nonlinear dc component proportional to $E_0 E_1^2$. The latter one is calculated from Eqs. (1)-(4) using the perturbation theory by the nonlinear memory term $-\Gamma_{ijkl}[\hat{\Delta}(\mathbf{r}, t)]\Pi_{kl}(\mathbf{r}, t-T)$ with the shift $\hat{\Delta}$ and the momentum flux density $\hat{\Pi}$ corresponding to V_0 and V_1 [47].

In Fig. 1(b,c) we draw the calculated profiles of the ac component of the flow $V_1(y)$ and the nonlinear dc component $V_\omega(y)$ in a sample being much wider than the wavelength of transversal magnetosound l_s . For such sample, the ac component $V_1(y)$ is formed by standing magnetosonic waves. The ac-field-induced correction $V_\omega(y)$ inherits both the oscillations of $V_1(y)$ and the parabolic profile of the linear dc response $V_0(y)$ [47].

In Fig. 2 we present the averaged photoconductivity $\Delta\sigma_\omega = \Delta I_\omega / (WE_0)$ multiplied on -1 . This value is proportional to the linear-in- \mathcal{W} photoresistivity $\Delta\rho_\omega = -\Delta\sigma_\omega / \sigma_0^2$. Here $\Delta I_\omega = en_0 \int_{-W/2}^{W/2} dy V_\omega(y)$ is the radiation-induced correction to the dc current I_0 and $\sigma_0 = I_0 / (WE_0)$ is the dc averaged conductivity. The curves are plotted at a fixed ac frequency ω and the sample widths W smaller, comparable, and larger than the characteristic decay length L_s . The dependence $-\Delta\sigma_\omega(\omega_c)$ exhibits the modulated oscillations by the inverse magnetic field, which are very similar to MIRO. The shape of the obtained oscillations is sinusoidal in the limiting cases $W \gg L_s$ and $W \ll L_s$, while for intermediate sample widths, $W \sim L_s$, it is irregular. The last property is related to the magnetosonic resonances in the ac linear response $V_1(y, t)$ [23]. Such resonances, being characteristic for highly viscous fluid, appear when a half-integer number of magnetosound wavelengths are placed inside the sample. They can be more or less sharp depending on parameters $\omega\tau_2$ and W/L_s [47].

4. *Discussion.* The obtained photoconductivity $\Delta\sigma_\omega$ does not depend on the sign “ \pm ” of the circular polarization of the radiation field $\mathbf{E}_1(t)$, unlike the photoresistance due to the memory effects and other mechanisms in disordered Ohmic samples [22, 30]. Indeed, for the considered here flow in a narrow sample ($W \ll l_p$), the ac linear response $V_1(y, t)$ is mainly formed by the viscoelastic contribution V_s . It is independent of the polarization sign \pm as the screening of the y component of the incident field $\mathbf{E}_1(t)$ by the internal field $\mathbf{E}^{int} \sim \delta n$ obligatory takes place at such W [23]. The nonlinear part of the velocity, V_ω stems from the memory term in Eqs. (2). The last one depends on the mismatch of the strain tensor, $\hat{\Delta}(\mathbf{r}, t) = \hat{\varepsilon}(\mathbf{r}, t) - \hat{\varepsilon}(\mathbf{r}, t - T)$, calculated by Eq. (1) for the linear response $V_{lin} = V_0 + V_1$. Thus V_ω is also independent of the sign \pm . For Ohmic flows in wide bulk samples, as it was implied in Ref. [22] and other theories, the ac electric field acting on electrons is just the external radiation field $\mathbf{E}_1(t)$. The relaxation memory term due to extended collisions of electrons with localized defects appears in the motion equation for the mean velocity $\mathbf{V}(t)$. Unlike the current hydrodynamic model, the defect-induced memory term contains the mismatch of the electron trajectories $\mathbf{r}_0(t)$, $\Delta(t) = \mathbf{r}_0(t) - \mathbf{r}_0(t - T)$. Such $\Delta \neq 0$ arises due to the force $e\mathbf{E}_0 + e\mathbf{E}_1(t)$ acting on electrons between their collisions with defects. Obviously, $\Delta(t)$ and the resulting photoconductivity strongly depend on the sign \pm of the polarization of $\mathbf{E}_1(t)$ [22, 30].

The obtained independence of the values $\Delta\sigma_\omega$ and $\Delta\rho_\omega$ on the polarization sign \pm and the appearance of an irregular shape of their oscillations with ω_c were observed in experiments [15, 16] on record-mobility GaAs quantum wells, but remained unexplained within theories [17–22] based on the model of independent electrons in bulk disordered samples [33, 34]. In [47] we cite and discuss

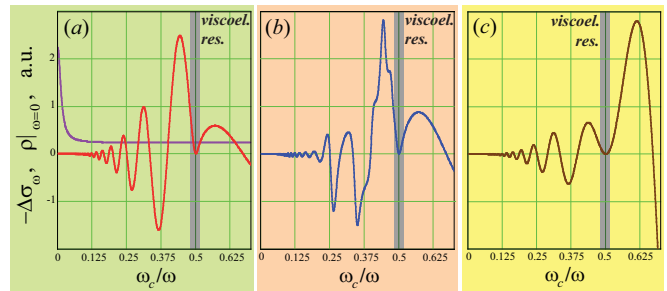


FIG. 2: Photoconductivity with the inverse sign, $-\Delta\sigma_\omega$, for Poiseuille flows of the fluid with the parameters $\omega\tau_2 = 40$; $\tau_q/\tau_2 = 0.7$ in long defectless samples with different widths $W/L_s = 6, 1.19, 0.03$ [red, blue, and brown curves in panels (a-c), respectively]. Grey stripes schematically denote the region near the viscoelastic resonance, $\omega = 2\omega_c$, where the fluid dynamics is dissipative in the main approximation and the developed theory is not applicable. In panel (a) we also plotted the dc magnetoresistance $\rho|_{\omega=0}(\omega_c)$ (violet curve) for a sample with the same parameters of the electron fluid and some density of defects. Such magnetoresistance consists of the two contributions [13]: the hydrodynamic one, proportional to $\eta_{xx} \sim (1 + 4\omega_c^2\tau_2^2)^{-1}$ and dominating at $\omega_c\tau_2 \lesssim 1$ ($\omega_c/\omega \lesssim 0.05$), and the Ohmic one, proportional to the rate of the scattering of quasiparticles on impurities, $1/\tau_{imp}$, and dominating at $\omega_c\tau_2 \gg 1$ ($\omega_c/\omega \gg 0.05$).

experimental data from [15, 16] and present some other properties of the calculated photoconductivity.

In [47] we also consider how the violation of the described above conditions of applicability of the highly viscous fluid model affects the hydrodynamic transport regime and the resulting photoresistance. Below we present the main conclusions of that consideration.

One of these conditions is the absence of bulk disorder. At $\omega_c \gg 1/\tau_2$ the hydrodynamic resistivity strongly decreases and the main contribution to the dc current I_0 can become the Ohmic one, provided some density of defects presents in a sample. This contribution is related to the scattering of quasiparticles on defects in the central part of the sample {the magnetoresistance for such samples is shown in Fig. 2(a); see Ref. [13] for the evidences of its realization in GaAs quantum wells}. At the same time, the viscoelastic part dominates in the ac flow component V_1 in not too wide samples, until $W \lesssim l_p$ [23]. Thus the predicted magnetooscillation of $\Delta\sigma_\omega$ due to the memory effect in the interparticle scattering can persist under certain conditions [47], originating now from the near-edge layers where both the dc and the ac flow components are still controlled by viscosity and viscoelasticity.

Another of these conditions is the very high non-ideality of the fluid. Similarly as for the qualitative applicability of equations (2) without the memory term for a moderately non-ideal electron fluid ($F_m \sim 1$), the current model of MIRO due to the memory effects in interparticle collisions, apparently, also remains qualitatively applicable for inhomogeneous flows of such fluid. Here-

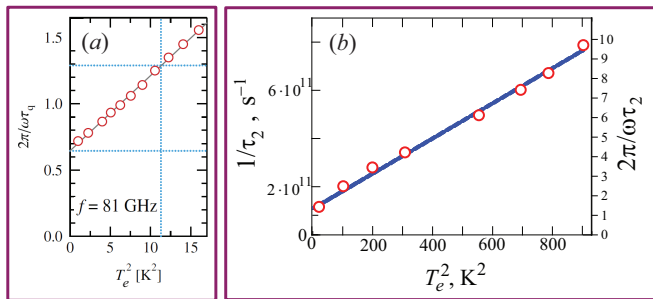


FIG. 3: (a) Experimental data on the departure scattering time τ_q as a function of temperature T_e , obtained from the measurements of the amplitude of MIRO in a high-mobility GaAs quantum well with the 2D electron density $n_0 = 2.8 \cdot 10^{11} \text{ cm}^{-2}$ ($r_s = 1.05$). Thin solid line is the quadratic fit $a + bT_e^2$. The picture is taken from Ref. [46]. (b) Shear stress relaxation time τ_2 at different T_e obtained from fitting of the giant negative magnetoresistance measured in Ref. [12] in a high-mobility GaAs/AlGaAs quantum well with the same n_0 . Blue solid line is the quadratic fit $a' + b'T_e^2$. Right vertical scale shows the values $1/\tau_2$ in the same units as in panel (a) [i. e., divided by the ac frequency on panel (a)].

with in order to precisely calculate V_0 , V_1 , and V_ω , the kinetic equation with a retarded collision operator should be used instead of hydrodynamic equations (2). The resulting photoresistance are to be still independent of the polarization sign at $W \ll l_p$ and its amplitude seems to be proportional to the same probability $P = e^{-T/\tau_q}$ for a quasiparticle to make a rotation without collisions.

In this connection, we present in Fig. 3 the experimental data for the two GaAs quantum wells with the same electron density n_0 corresponding to the intermediate interaction parameter $r_s = 1.05$ and, thus, to the moderately large Landau parameters $F_m \sim 1$. In panel (a) we cite the data on the departure scattering time $\tau_q(T_e)$ obtained in Ref. [46] from the measurements of the temperature dependence of the MIRO amplitude, which was supposed to be proportional to $P = e^{-T/\tau_q}$. In panel (b) we plot experimental data on the shear stress relaxation time $\tau_2(T_e)$ extracted by us from the giant negative magnetoresistance measured in Ref. [12] using the method of fitting from Refs. [13, 42]. Both the rates $1/\tau_q$ and $1/\tau_2$ are approximately quadratic with the electron temperature T_e and have some residual values in the limit $T_e \rightarrow 0$ (see discussion in [47]). The temperature-dependent part of τ_q is in several times shorter than the one of τ_2 , that is in a qualitative agreement with the calculations of these times at $r_s \sim 1$ within the kinetic equation [41].

Such agreement between the data in Figs. 3(a) and 3(b) evidences in favor of the hydrodynamic nature of the MIRO in some high-mobility GaAs quantum wells with a moderately strong interparticle interaction, where the giant negative magnetoresistance signify the formation of an inhomogeneous viscous electron flow and the developed model is to be qualitatively applicable.

5. *Conclusion.* We have shown that the flow of a highly viscous 2D electron fluid in the presence of microwave radiation exhibits magnetooscillations of photoconductivity. Such oscillations are due to (i) the near-elastic dynamics of the ac component of the flow and (ii) the memory effects in inter-particle scattering in a magnetic field. The calculated photoconductivity and photoresistance coincides by many properties with MIRO observed in best-quality GaAs quantum wells. The obtained result evidences that 2D electrons in the best-quality GaAs quantum wells in moderate magnetic fields form a highly viscous fluid. This highly correlated electron phase seems to be a moderate-field precursor of the Laughlin liquid in the fraction quantum Hall regime.

We thank M. I. Dyakonov for numerous discussions of transport experiments on high-mobility electron systems that led to this work, as well as for discussions of some of the issues raised in this work, for reading the preliminary version of the manuscript, and kind advices how to improve it. We also thank A. P. Dmitriev and Y. M. Bel-tukov for fruitful discussions. One of us (P. S. A.) thanks E. G. Alekseeva, I. P. Alekseeva, N. S. Averkiev, K. A. Baryshnikov, K. S. Denisov, I. V. Krainov, and S. M. Postolov for kind advise and support.

This work was financially supported by the Russian Science Foundation (Grant No. 18-72-10111).

-
- [1] L. Levitov and G. Falkovich, Electron viscosity, current vortices and negative nonlocal resistance in graphene, *Nature Physics* **12**, 672 (2016).
 - [2] D. A. Bandurin, I. Torre, R. Krishna Kumar, M. Ben Shalom, A. Tomadin, A. Principi, G. H. Auton, E. Khestanova, K. S. Novoselov, I. V. Grigorieva, L. A. Ponomarenko, A. K. Geim, and M. Polini, Negative local resistance caused by viscous electron backflow in graphene, *Science* **351**, 1055 (2016).
 - [3] R. Krishna Kumar, D. A. Bandurin, F. M. D. Pellegrino, Y. Cao, A. Principi, H. Guo, G. H. Auton, M. Ben Shalom, L. A. Ponomarenko, G. Falkovich, K. Watanabe, T. Taniguchi, I. V. Grigorieva, L. S. Levitov, M. Polini, and A. K. Geim, Superballistic flow of viscous electron fluid through graphene constrictions, *Nature Physics* **13**, 1182 (2017).
 - [4] J. A. Sulpizio, L. Ella, A. Rozen, J. Birkbeck, D. J. Perello, D. Dutta, M. Ben-Shalom, T. Taniguchi, K. Watanabe, T. Holder, R. Queiroz, A. Principi, A. Stern, T. Scaffidi, A. K. Geim, and S. Ilani, Visualizing Poiseuille flow of hydrodynamic electrons, *Nature* **576**, 75 (2019).
 - [5] M. J. H. Ku, T. X. Zhou, Q. Li, Y. J. Shin, J. K. Shi, C. Burch, L. E. Anderson, A. T. Pierce, Y. Xie, A. Hamo, U. Vool, H. Zhang, F. Casola, T. Taniguchi, K. Watanabe, M. M. Fogler, P. Kim, A. Yacoby,

- and R. L. Walsworth, Imaging viscous flow of the Dirac fluid in graphene, *Nature* **583**, 537 (2020).
- [6] M. Polini and A. Geim, Viscous electron fluids, *Physics Today* **73**, 6, 28 (2020).
- [7] P. J. W. Moll, P. Kushwaha, N. Nandi, B. Schmidt, and A. P. Mackenzie, Evidence for hydrodynamic electron flow in PdCoO₂, *Science* **351**, 1061 (2016).
- [8] J. Gooth, F. Menges, C. Shekhar, V. Suess, N. Kumar, Y. Sun, U. Drechsler, R. Zierold, C. Felser, and B. Gotsmann, Thermal and electrical signatures of a hydrodynamic electron fluid in tungsten diphosphide, *Nature Communications* **9**, 4093 (2018).
- [9] A. T. Hatke, M. A. Zudov, J. L. Reno, L. N. Pfeiffer, and K. W. West, Giant negative magnetoresistance in high-mobility two-dimensional electron systems, *Phys. Rev. B* **85**, 081304 (2012).
- [10] R. G. Mani, A. Kriisa, and W. Wegscheider, Size-dependent giant-magnetoresistance in millimeter scale GaAs/AlGaAs 2D electron devices, *Scientific Reports* **3**, 2747 (2013).
- [11] L. Bockhorn, P. Barthold, D. Schuh, W. Wegscheider, and R. J. Haug, Magnetoresistance in a high-mobility two-dimensional electron gas, *Phys. Rev. B* **83**, 113301 (2011).
- [12] Q. Shi, P. D. Martin, Q. A. Ebner, M. A. Zudov, L. N. Pfeiffer, and K. W. West, Colossal negative magnetoresistance in a two-dimensional electron gas, *Phys. Rev. B* **89**, 201301 (2014).
- [13] P. S. Alekseev, Negative magnetoresistance in viscous flow of two-dimensional electrons, *Phys. Rev. Lett.* **117**, 166601 (2016).
- [14] G. M. Gusev, A. D. Levin, E. V. Levinson, and A. K. Bakarov, Viscous electron flow in mesoscopic two-dimensional electron gas, *AIP Advances* **8**, 025318 (2018).
- [15] J. H. Smet, B. Gorshunov, C. Jiang, L. Pfeiffer, K. West, V. Umansky, M. Dressel, R. Meisels, F. Kuchar, and K. von Klitzing, circular-polarization-dependent study of the microwave photoconductivity in a two-dimensional electron system, *Phys. Rev. Lett.* **95**, 116804 (2005).
- [16] T. Herrmann, I. A. Dmitriev, D. A. Kozlov, M. Schneider, B. Jentzsch, Z. D. Kvon, P. Olbrich, V. V. Belkov, A. Bayer, D. Schuh, D. Bougeard, T. Kuczmik, M. Oltcher, D. Weiss, and S. D. Ganichev, Analog of microwave-induced resistance oscillations induced in GaAs heterostructures by terahertz radiation, *Phys. Rev. B* **94**, 081301 (2016).
- [17] A. C. Durst, S. Sachdev, N. Read, and S. M. Girvin, Radiation-induced magnetoresistance oscillations in a 2D electron gas, *Phys. Rev. Lett.* **91**, 086803 (2003).
- [18] M. G. Vavilov and I. L. Aleiner, Magnetotransport in a two-dimensional electron gas at large filling factors, *Phys. Rev. B* **69**, 035303 (2004).
- [19] I. A. Dmitriev, A. D. Mirlin, and D. G. Polyakov, Cyclotron-resonance harmonics in the ac response of a 2D electron gas with smooth disorder, *Phys. Rev. Lett.* **91**, 226802 (2003).
- [20] I. A. Dmitriev, M. G. Vavilov, I. L. Aleiner, A. D. Mirlin, and D. G. Polyakov, Theory of microwave-induced oscillations in the magnetoconductivity of a 2D electron gas, *Phys. Rev. B* **71**, 115316 (2005).
- [21] I. A. Dmitriev, A. D. Mirlin, and D. G. Polyakov, Oscillatory ac conductivity and photoconductivity of a two-dimensional electron gas: Quasiclassical transport beyond the Boltzmann equation, *Phys. Rev. B* **70**, 165305 (2004).
- [22] Y. M. Beltukov and M. I. Dyakonov, Microwave-induced resistance oscillations as a classical memory effect, *Phys. Rev. Lett.* **116**, 176801 (2016).
- [23] P. S. Alekseev and A. P. Alekseeva, Transverse magnetosonic waves and viscoelastic resonance in a two-dimensional highly viscous electron fluid, *Phys. Rev. Lett.* **123**, 236801 (2019).
- [24] Y. Dai, R. R. Du, L. N. Pfeiffer, and K. W. West, Observation of a cyclotron harmonic spike in microwave-induced resistances in ultraclean GaAs/AlGaAs quantum wells, *Phys. Rev. Lett.* **105**, 246802 (2010).
- [25] A. T. Hatke, M. A. Zudov, L. N. Pfeiffer, and K. W. West, Giant microwave photoresistivity in high-mobility quantum Hall systems, *Phys. Rev. B* **83**, 121301 (2011).
- [26] M. Bialek, J. Lusakowski, M. Czapkiewicz, J. Wrobel, and V. Umansky, Photoresponse of a two-dimensional electron gas at the second harmonic of the cyclotron resonance, *Phys. Rev. B* **91**, 045437 (2015).
- [27] M. A. Zudov, R. R. Du, J. A. Simmons, and J. L. Reno, Shubnikov-de Haas-like oscillations in millimeterwave photoconductivity in a high-mobility two-dimensional electron gas, *Phys. Rev. B* **64**, 201311 (2001).
- [28] P. D. Ye, L. W. Engel, D. C. Tsui, J. A. Simmons, J. R. Wendt, G. A. Vawter, and J. L. Reno, Giant microwave photoresistance of two-dimensional electron gas, *Appl. Phys. Lett.* **79**, 2193 (2001).
- [29] R. G. Mani, J. H. Smet, K. von Klitzing, V. Narayana-murti, W. B. Johnson, and V. Umansky, Zero-resistance states induced by electromagnetic-wave excitation in GaAs/AlGaAs heterostructures, *Nature* **420**, 646 (2002).
- [30] I. A. Dmitriev, A. D. Mirlin, D. G. Polyakov, and M. A. Zudov, Nonequilibrium phenomena in high Landau levels, *Rev. Mod. Phys.* **84**, 1709 (2012).
- [31] V. I. Ryzhii, Photoconductivity characteristics in thin

- films subjected to crossed electric and magnetic fields, *Sov. Phys. Solid State* **11**, 2078 (1970).
- [32] V. I. Ryzhii, R. A. Suris, and B. S. Shchamkhalova, Photoconductivity of a two-dimensional electron gas in a strong magnetic field, *Sov. Phys. Semicond.* **20**, 1299 (1987).
- [33] In Ref. [30] the following idea about the explanation of the absence of the dependence of MIRO on the sign of the circular polarization of an incident radiation field $\mathbf{E}_1^{ext}(t)$ was formulated. The difference of the polarization of the actual ac field $\mathbf{E}_1(\mathbf{r}, t) = \mathbf{E}_1^{ext}(t) + \mathbf{E}_1^{int}(\mathbf{r}, t)$, which is “felt” by 2D electrons, from the polarization of the incident field $\mathbf{E}_1^{ext}(t)$ can be induced by some elements of an experimental setup and can result in the independence of MIRO on the sign of the polarization of $\mathbf{E}_1^{ext}(t)$. However, it was not indicated in Ref. [30] that this modification of the polarization can be a consequence of the screening of one of the components of the incident field $\mathbf{E}_1^{ext}(t)$ by the internal ac field $\mathbf{E}_1^{int}(\mathbf{r}, t)$ originating from the redistribution of the very 2D electron fluid density $\delta n(\mathbf{r}, t)$ and can be inextricably related with the mechanism of MIRO.
- [34] In Refs. [35, 36] theories of another type for the 2D electron magnetotransport were developed, in which the photoresistance is associated with the ac-field-induced redistribution of the electron density in sample contacts [35] or near localized defects in a sample [36]. Although these theories lead to magnetos oscillations of photoresistance with a weak dependence on the sign of the circular polarization of the incident radiation, there exist substantial problems in the comparison of other predictions of those theories with experiments on MIRO. For example, there is a discrepancy between the shapes of the predicted oscillations and of the oscillations observed in experiments. The latter ones are often sinusoidal, whereas in Refs. [35, 36] such shape of magnetooscillations was not obtained.
- [35] S. A. Mikhailov, Theory of microwave-induced zero-resistance states in two-dimensional electron systems, *Phys. Rev. B* **83**, 155303 (2011).
- [36] A. D. Chepelianskii and D. L. Shepelyansky, Floquet theory of microwave absorption by an impurity in the two-dimensional electron gas, *Phys. Rev. B* **97**, 125415 (2018).
- [37] Similar hydrodynamic mechanism for negative magnetoresistance was proposed many years ago for bulk ultra-pure metals in publication: R. P. Gurzhi and S. I. Shevchenko, Hydrodynamic mechanism of electric conductivity of metals in a magnetic field, *Soviet Physics JETP* **27**, 1019 (1968).
- [38] P. S. Alekseev, Magnetic resonance in a high-frequency flow of a two-dimensional viscous electron fluid, *Phys. Rev. B* **98**, 165440 (2018).
- [39] S. Conti and G. Vignale, Elasticity of an electron liquid, *Phys. Rev. B* **60**, 7966 (1999).
- [40] P. S. Alekseev, Magnetosonic Waves in a Two-Dimensional Electron Fermi Liquid, *Semiconductors* **53**, 1367 (2019).
- [41] D. S. Novikov, Viscosity of a two-dimensional Fermi liquid, arXiv:cond-mat/0603184 (2006).
- [42] P. S. Alekseev and A. P. Dmitriev, Viscosity of two-dimensional electrons, *Phys. Rev. B* **102**, 241409 (2020).
- [43] E. M. Baskin, L. N. Magarill, and M. V. Entin, Twodimensional electron-impurity system in a strong magnetic field, *Sov. Phys. JETP* **48**, 365 (1978).
- [44] A. V. Bobylev, F. A. Maa, A. Hansen, and E. H. Hauge, Two-dimensional magnetotransport according to the classical Lorentz model, *Phys. Rev. Lett.* **75**, 197 (1995).
- [45] A. Dmitriev, M. Dyakonov, and R. Jullien, Classical mechanism for negative magnetoresistance in two dimensions, *Phys. Rev. B* **64**, 233321 (2001).
- [46] A. T. Hatke, M. A. Zudov, L. N. Pfeiffer, and K. W. West, Temperature dependence of microwave photoresistance in 2D electron systems, *Phys. Rev. Lett.* **102**, 066804 (2009).
- [47] See Supplemental information below, containing additional references [48]-[54], for details of calculations, and comparison with experiments.
- [48] V. V. Cheianov, A. P. Dmitriev, and V. Yu. Kachorovskii, Non-Markovian effects on the two-dimensional magnetotransport: low-field anomaly in magnetoresistance, *Phys. Rev. B* **70**, 245307 (2004).
- [49] Y. M. Beltukov, private communication.
- [50] S. A. Studenikin, A. S. Sachrajda, J. A. Gupta, Z. R. Wasilewski, O. M. Fedorych, M. Byszewski, D. K. Maude, M. Potemski, M. Hilke, K. W. West and L. N. Pfeiffer, Frequency quenching of microwave-induced resistance oscillations in a high-mobility two-dimensional electron gas, *Phys. Rev. B* **76**, 165321 (2007).
- [51] S. Wiedmann, G. M. Gusev, O. E. Raichev, A. K. Bakarov, and J. C. Portal, Crossover between distinct mechanisms of microwave photoresistance in bilayer systems, *Phys. Rev. B* **81**, 085311 (2010).
- [52] J. Y. Khoo and I. S. Villadiego, Shear sound of two-dimensional Fermi liquids, *Phys. Rev. B* **99**, 075434 (2019).
- [53] L. Bockhorn, I. V. Gornyi, D. Schuh, C. Reichl, W. Wegscheider, and R. J. Haug, Magnetoresistance induced by rare strong scatterers in a high-mobility two-dimensional electron gas, *Phys. Rev. B* **90**, 165434 (2014).
- [54] E. M. Lifshitz and L. P. Pitaevskii, *Statistical Physics*, 1st ed. (Pergamon Press, Oxford, 1981).

Supplementary information to “Microwave-induced resistance oscillations in highly viscous electron fluid”

P. S. Alekseev and A. P. Alekseeva

Ioffe Institute, Politekhnikeskaya 26, 194021, St. Petersburg, Russia

Here we present the details of our theoretical model, of the solution of its equations, and of derivation of the properties of the resulting photoconductivity. We also discuss possible extensions of our theoretical model to more general systems and compare our results with preceding theoretical and experimental works.

1. Memory effects in ac flow of highly viscous 2D electron fluid

Memory effects in classical ac magnetotransport of non-interacting 2D electrons in disordered samples were considered, for example, in Refs. [21, 22, 43–45, 48].

For the scattering of 2D electrons on defects with a localized potential (“impurities”), the memory effects in a perpendicular magnetic field \mathbf{B} are due to the appearance of (i) the electrons not scattering on defects (their trajectories are located between the impurities) and of (ii) the so-called “extended collisions”. The last events consist of several returns of an electron to the same impurity after a first scattering on it because of cyclotron rotation (see Fig. 2 in Ref. [22]). Both these effects (i) and (ii) become substantial in the classically strong magnetic fields, when the electron mean free path relative to the scattering on defects becomes comparable with the length of the cyclotron circle [43].

Within the approach of Ref. [22], such events are accounted in a phenomenological physically transparent way by the retardation term $-\hat{\Gamma}(t)\mathbf{V}(t-T)$ in the Drude-like equation for the mean velocity $\mathbf{V}(t)$:

$$\frac{\partial \mathbf{V}}{\partial t} = \frac{e}{m} \mathbf{E}(t) + [\mathbf{V} \times \boldsymbol{\omega}_c] - (1-P) \left[\frac{\mathbf{V}}{\tau_{tr}} + \hat{\Gamma}(t) \mathbf{V}(t-T) \right], \quad (\text{S1})$$

where e and m are the electron charge and the electron mass, the electric field $\mathbf{E}(t)$ can contain dc and ac components; $\boldsymbol{\omega}_c = \omega_c \mathbf{e}_z$ is the vector along the magnetic field, $\omega_c = eB/(mc)$ is the electron cyclotron frequency, τ_{tr} is the momentum relaxation time due to the scattering on disorder in the absence of the memory effect,

$$P = e^{-T/\tau_q} \quad (\text{S2})$$

is the probability for an electron to make a full cyclotron rotation without collisions with defects, τ_q is the departure scattering time due to collisions with defects, $T = 2\pi/\omega_c$ is the cyclotron period, and $\hat{\Gamma}(t)$ is the retarded relaxation tensor due to double extended collisions.

The tensor $\hat{\Gamma}(t)$ depends on the dynamics of individual electrons in the past, $t' < t$. At sufficiently weak flows, such dependence is accounted by a nonlinear contributions in $\hat{\Gamma}$ [being additional to the unperturbed value $\hat{\Gamma}^{(0)}$ corresponding to the limit $E, V \rightarrow 0$]. This contribution is proportional to some values characterizing the deviation of the electron trajectories $\mathbf{r}_0(t)$ from the exact cyclotron circles:

$$\Gamma_{ij}(\boldsymbol{\Delta}) = \Gamma_{ij}^{(0)} + \alpha \Delta^2 \delta_{ij} + \beta \Delta_i \Delta_j. \quad (\text{S3})$$

Here the coefficients $\hat{\Gamma}^{(0)}$, α , and β are the microscopic characteristics of the electron gas and the defects, being proportional to the probability P (S2), and the value Δ is the mismatch $\boldsymbol{\Delta}(t) = \boldsymbol{\rho}(t) - \boldsymbol{\rho}(t-T)$ of the impact scattering parameters $\boldsymbol{\rho}(t) = \mathbf{r}_0(t) - \mathbf{R}_0$ and $\boldsymbol{\rho}(t-T) = \mathbf{r}_0(t-T) - \mathbf{R}_0$ of an electron in two successive collisions with the same defect [here \mathbf{R}_0 is the position of the defect center; it follows from the above formulas that $\boldsymbol{\Delta}(t) = \mathbf{r}_0(t) - \mathbf{r}_0(t-T)$]. Such form (S3) of the contribution in $\hat{\Gamma}$ from the perturbation of the trajectories between collisions is valid when the size of defects is small: $a \ll R_c$. Provided this inequality, the mismatch $\boldsymbol{\Delta}(t)$ is directly related with the forces from the dc and the ac electric fields \mathbf{E}_0 and $\mathbf{E}_1(t)$ acting on an electron during a cyclotron period $t-T < t' < t$. Herewith in the approximation linear by \mathbf{E}_0 and $\mathbf{E}_1(t)$, the corresponding value of the mismatch:

$$\boldsymbol{\Delta}(t) = \boldsymbol{\Delta}_0 + \boldsymbol{\Delta}_1(t), \quad (\text{S4})$$

does not depend on particular parameters of a trajectory $\mathbf{r}_0(t)$.

Such model allowed to analytically calculate the photoconductivity of non-interacting 2D electrons in bulk samples [22]. The obtained magnetooscillations of the photoconductivity are induced by the described extended collisions and are similar in many properties to the ones of MIRO observed in experiments.

In this work we formulate and solve similar phenomenological dynamic equations for the case of 2D interacting electrons forming a highly viscous fluid in samples with no defects (or, more generally, in the sample

regions where defects are not substantial for the flow). The formulated model accounts the viscosity and the viscoelasticity effects in the ac and the dc components of a flow, respectively, as well as the memory effect in collisions between quasiparticles of the fluid. We will see that such model also leads to magnetooscillations in photoresistance, coinciding in many properties with MIRO.

For a viscous electron fluid, the motion equation must describe not only of the mean velocity $\mathbf{V}(\mathbf{r}, t)$, being now inhomogeneous by \mathbf{r} , but also the perturbed electron density $n(\mathbf{r}, t)$ and the shear stress tensor $\hat{\Pi}(\mathbf{r}, t)$. The hydrodynamic equations of evolution of these values for a highly viscous 2D electron fluid without accounting for the memory effects were formulated and derived in Refs. [13, 23, 38–40, 42]. For the case a high-frequency flow, those equations are transformed into Hooke's equations of an almost elastic dynamics of an electron media with a weak damping due to interparticle scattering [39, 40]. In Hooke's equations, the value that describes the state of the system is the displacement vector $\mathbf{u}(\mathbf{r}, t)$, related to the strain tensor $\varepsilon_{ij}(\mathbf{r}, t)$. In this work it is convenient to define ε_{ij} as:

$$\varepsilon_{ij} = \frac{\partial u_i}{\partial x_j} + \frac{\partial u_j}{\partial x_i}. \quad (\text{S5})$$

The connection between Hooke's and the Navier-Stokes equations is based on relation (M1) for the hydrodynamic velocity in an almost elastic flow of the fluid:

$$\mathbf{V}(\mathbf{r}, t) \approx \frac{\partial \mathbf{u}(\mathbf{r}, t)}{\partial t}. \quad (\text{S6})$$

This formula describes the absence of slipping between neighbor layers of the flow. Here and below the references (M1)-(M3) denote the equations in the main text.

Generally, the dynamics of a viscous fluid with taking into account the interparticle scattering, resulting in slipping between fluid layers, is described by the full set of the hydrodynamic variables: the density n , the velocity \mathbf{V} , and the shear stress tensor Π_{ij} [38]. Equation (S6) in this case is a formula for calculation, in the linear by \mathbf{V} approximation, of the displacement $\mathbf{u}(\mathbf{r}, t)$ of fluid elements. Note that \mathbf{u} for a flow with the slipping of neighbour layers is not the variable sufficient for the description of the fluid dynamics.

Analogously to the dynamics of independent electrons in a sample with small-size defects, the memory effect for an electron fluid in a defectless sample in a magnetic field is due to the "extended collisions" between electron-like Fermi-liquid quasiparticles (see Fig. S1 and Fig. 1 in the main text). Indeed, if the mean free path of quasiparticles relative to their collisions is of the order or larger than the length of the cyclotron circle $2\pi R_c$, two quasiparticles can suffer several successive collisions with slow step-like changing of their relative impact scattering parameter $\varrho(t) = \mathbf{r}_{0,1}(t) - \mathbf{r}_{0,2}(t)$ (see Fig. S1). This leads

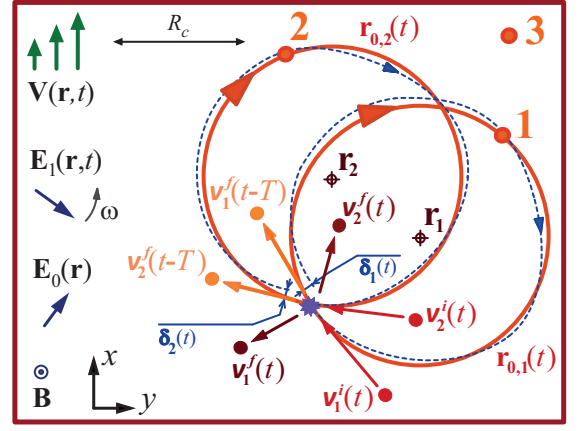


FIG. S1: Sketch of the microscopic mechanism of the memory effect in collisions of electron-like quasiparticles in a 2D electron Fermi-liquid in a classical magnetic field $\mathbf{B} = B\mathbf{e}_z$. Motion of the fluid, averaged by dynamics of quasiparticles, is described by the hydrodynamic velocity $\mathbf{V}(\mathbf{r}, t)$. It contains the components which are linear by the applied electric fields, $\mathbf{V}_0(\mathbf{r}) \sim \mathbf{E}_0$ and $\mathbf{V}_1(\mathbf{r}, t) \approx \partial \mathbf{u}(\mathbf{r}, t) / \partial t \sim \mathbf{E}_1(t)$, and nonlinear by \mathbf{E}_0 and $\mathbf{E}_1(t)$ components. Red solid lines are the quasiparticle trajectories at $\mathbf{E}_0, \mathbf{E}_1, \mathbf{V} \equiv 0$, which are exact cyclotron circles. Blue dashed lines are the trajectories accounting the elastic force, microscopically related to space-dependent perturbations of the quasiparticle energy spectrum and leading to the term $\sim V_{ij}(\mathbf{r}, t)$ in Eq. (S7), as well as to the forces from the full dc and the ac fields $\mathbf{E}_0(\mathbf{r}, t)$ and $\mathbf{E}_1(\mathbf{r}, t)$ (S8). The profiles of $\mathbf{V}(\mathbf{r}, t)$ and $\mathbf{u}(\mathbf{r}, t)$ are changing weakly by \mathbf{r} on the scale of R_c . The value of the relative impact scattering parameter, $\varrho(t') = \mathbf{r}_{0,1}(t') - \mathbf{r}_{0,2}(t')$, at the moment $t' = t - T$ differ from its value at $t' = t$ on the difference $\delta(t) = \delta_1(t) - \delta_2(t)$ of the trajectory mismatches by a period $\delta_p(t) = \mathbf{r}_{0,p}(t) - \mathbf{r}_{0,p}(t - T)$, $p = 1, 2$. The values $\delta_p(t)$ are estimated as the mean shifts of the whole fluid in the centers \mathbf{r}_p by a period: $\delta_p(t) \sim [\mathbf{u}(\mathbf{r}_p, t) - \mathbf{u}(\mathbf{r}_p, t - T)]$.

to the dependence of the rate of relaxation of the shear stress, $\partial \hat{\Pi} / \partial t$, in the moment t on the characteristic of the fluid in the moments of previous scattering events in the extended collisions, $t - mT$, where $m = 1, 2, \dots$ is a number of successive rotations in an extended collision.

The phenomenological dynamic equations for a highly viscous 2D electron fluid accounting the double extended collisions ($m = 1$) are equations (M2) in the main text:

$$\left\{ \begin{array}{l} \frac{\partial n}{\partial t} + n_0 \operatorname{div} \mathbf{V} = 0 \\ \frac{\partial V_i}{\partial t} = \frac{e}{m} E_i(\mathbf{r}, t) + \omega_c \epsilon_{ikz} V_k - \frac{1}{m} \frac{\partial \Pi_{ij}}{\partial x_j} \\ \frac{\partial \Pi_{ij}}{\partial t} = \omega_c (\epsilon_{ikz} \Pi_{kj} + \epsilon_{jkz} \Pi_{ik}) - \frac{m(v_F^n)^2}{4} V_{ij} \\ \quad - \frac{\Pi_{ij}}{\tau_2} - \Gamma_{ijkl}(\mathbf{r}, t) \Pi_{kl}(\mathbf{r}, t - T) \end{array} \right. \quad (\text{S7})$$

Here $n_0 = n - \delta n$ is the equilibrium fluid density; the

electric field $\mathbf{E}(\mathbf{r}, t)$ contains the components from dc and ac external fields induced by the electric bias and the microwave radiation as well as from the internal the dc and ac field related to the non-equilibrium charge density $e \delta n(\mathbf{r}, t)$: $\mathbf{E}(\mathbf{r}, t) = \mathbf{E}_0(\mathbf{r}) + \mathbf{E}_1(\mathbf{r}, t)$, where

$$\begin{aligned} \mathbf{E}_0(\mathbf{r}) &= \mathbf{E}_0^{ext} + \mathbf{E}_0^{int}(\mathbf{r}), \\ \mathbf{E}_1(\mathbf{r}, t) &= \mathbf{E}_1^{ext}(t) + \mathbf{E}_1^{int}(\mathbf{r}, t); \end{aligned} \quad (\text{S8})$$

ϵ_{ikm} is the antisymmetric unit tensor; $V_{ij} = V_{ij}(\mathbf{r}, t)$ is the tensor of the gradients of the velocity \mathbf{V} :

$$V_{ij} = \frac{\partial V_i}{\partial x_j} + \frac{\partial V_j}{\partial x_i}; \quad (\text{S9})$$

τ_2 is the shear stress relaxation time without the memory effects; v_F^η is the parameter defining the magnitude of the viscosity η of a highly viscous fluid [23]:

$$\eta|_{B=0} = \frac{1}{4} (v_F^\eta)^2 \tau_2; \quad (\text{S10})$$

$\hat{\Gamma}_{ijkl}(\mathbf{r}, t)$ is the tensor describing the retarded relaxation of Π_{ij} due to the extended collisions (see Fig. S1); and $T = 2\pi/\omega_c$ is the cyclotron period.

In the latter equation of system (S7) we omit the factor $(1 - P)$ as we consider it to be close to unity [compare Eqs. (S1) and (S7)]; now P is the probability to make a full rotation without interparticle scattering]. In Ref. [40] the interaction-induced renormalization of the parameters in Eq. (S7) others than v_F^η were derived, but they are not substantial for the problem of the current study, therefore we also omit them here.

We suppose that the characteristic radius of the interparticle interaction potential is much smaller than the cyclotron radius. In this case, each extended collision consists of two (or several) successive collisions of two quasiparticles in a small region (a blue star in Fig. S1) and of almost collisionless motions of these two quasiparticles far from the region of scattering. This motion is mainly determined by the magnetic field, but is also substantially affected by the full electric field $\mathbf{E}(\mathbf{r}, t)$ (S8) as well as by the elastic force, related to the space-dependent change of the quasiparticle energy spectrum [39, 40] and leading to the term $\sim V_{ij}(\mathbf{r}, t)$ in Eq. (S7). The elastic force and the components \mathbf{E}_0^{int} and \mathbf{E}_1^{int} of field (S8) are inhomogeneous by \mathbf{r} and are determined by the formation of the flow in the whole sample. Their space inhomogeneity leads to the difference of the full forces acting on two quasiparticles “1” and “2” (see Fig. S1). This difference defines the dependence of the probability of the extend collisions on the flow magnitude and shape.

To describe such memory effect microscopically, one should use the Boltzmann-like kinetic equation with a generalized collision operator of the inter-quasiparticle scattering, being nonlocal by time. Such collision operator, leading to the motion equation of the upper

Eqs. (S7), could be derived within some sophisticated procedure from the classical or the quantum Liouville equations for the interacting Fermi-liquid electron-like quasiparticles. Herewith some other retarded terms in the resulting effective transport equations, except the term $-\Gamma_{ijkl}(\mathbf{r}, t)\Pi_{kl}(\mathbf{r}, t - T)$ accounted in Eq. (S7), may be possible, for example: $A_{ij}E_j(\mathbf{r}, t - T)$, $B_{ijkl}E_j(\mathbf{r}, t - T)\Pi_{kl}(\mathbf{r}, t - T)$, and so on [49]. However we hope that the term $-\Gamma_{ijkl}(\mathbf{r}, t)\Pi_{kl}(\mathbf{r}, t - T)$ is sufficient to describe the main properties of the photoconductivity induced by the memory effect in interparticle collisions.

Quantitatively, the extended inter-particle collisions are characterized by the following values. Two successive collisions are controlled by the impact relative scattering parameter of particles “1” and “2” (see Fig. S1):

$$\boldsymbol{\varrho}(t') = \mathbf{r}_{0,1}(t') - \mathbf{r}_{0,2}(t'), \quad t' = t, t - T. \quad (\text{S11})$$

During one cyclotron period $t - T < t' < t$, two scattered quasiparticles are moving along the trajectories $\mathbf{r}_{0,1}(t)$ and $\mathbf{r}_{0,2}(t)$ with the centers near the points \mathbf{r}_1 and \mathbf{r}_2 . Their impact scattering parameter $\boldsymbol{\varrho}(t')$ (S11) differs in the moments $t' = t$ and $t' = t - T$ on the value $\boldsymbol{\delta}(t) = \boldsymbol{\delta}_1(t) - \boldsymbol{\delta}_2(t)$, where $\boldsymbol{\delta}_1(t)$ and $\boldsymbol{\delta}_2(t)$ are the mismatches of the trajectories $\mathbf{r}_{0,1}(t)$ and $\mathbf{r}_{0,2}(t)$ by a cyclotron period:

$$\begin{aligned} \boldsymbol{\delta}(t) &= \boldsymbol{\varrho}(t) - \boldsymbol{\varrho}(t - T) = \boldsymbol{\delta}_1(t) - \boldsymbol{\delta}_2(t), \\ \boldsymbol{\delta}_p(t) &= \mathbf{r}_{0,p}(t) - \mathbf{r}_{0,p}(t - T), \quad p = 1, 2. \end{aligned} \quad (\text{S12})$$

Nonzero values of the mismatches $\boldsymbol{\delta}_p(t)$ are induced by the action of the elastic force $V_{ij}(\mathbf{r}, t)$ and the electric fields (S8), as it was discussed above (see also Fig. S1).

In accordance with the essence of the extended collisions, the tensor $\Gamma_{ijkl}(\mathbf{r}, t)$ in the retarded relaxation term in Eq. (S7) is determined by the mismatches $\boldsymbol{\delta}(t)$ (S12) of the scattering parameters $\boldsymbol{\varrho}(t')$ (S11), averaged by all the quasiparticle pairs near the given point \mathbf{r} . The mean mismatch $\langle \boldsymbol{\delta}(t) \rangle$ is apparently expressed via the macroscopic variables of the fluid in the past, generally speaking, via all variables: n , \mathbf{V} , $\hat{\Pi}$. Thus the tensor $\Gamma_{ijkl}(\mathbf{r}, t)$ depends on these variables as an operator:

$$\Gamma_{ijkl}(\mathbf{r}, t) = \hat{\Gamma}_{ijkl}[n(\mathbf{r}', t'), \mathbf{V}(\mathbf{r}', t'), \hat{\Pi}(\mathbf{r}', t')], \quad (\text{S13})$$

where $|\mathbf{r} - \mathbf{r}'| \lesssim R_c$ and $t - T \lesssim t' < t$.

We suppose that interparticle scattering is weak ($\omega, \omega_c \gg 1/\tau_2$) and the system is far from the resonances ($|\omega - \omega_c| \gg 1/\tau_2$ and $|\omega - 2\omega_c| \gg 1/\tau_2$). In this case, a collision of one of two particles during an extended collision with a third particle is a rare event (see Fig. S1). Thus the only macroscopic variable determining the mismatches $\boldsymbol{\delta}_1(t)$ and $\boldsymbol{\delta}_2(t)$ is the displacement vector $\mathbf{u}(\mathbf{r}', t')$ in the centers of the particle trajectories “1” and “2” (see Fig. S1):

$$\boldsymbol{\delta}_p(t) \sim \mathbf{u}(\mathbf{r}_p, t) - \mathbf{u}(\mathbf{r}_p, t - T), \quad p = 1, 2. \quad (\text{S14})$$

For the resulting dependence of $\hat{\Gamma}$ on the shape and the magnitude of the flow we have:

$$\hat{\Gamma}_{ijkl}[\mathbf{u}(\mathbf{r}', t')] = \Gamma_{ijkl} \left(\langle \delta \mathbf{u}(\mathbf{r}_1, \mathbf{r}_2, t) \rangle_{\mathbf{r}_1, \mathbf{r}_2} \right), \quad (\text{S15})$$

where the brackets $\langle \cdot \rangle_{\mathbf{r}_1, \mathbf{r}_2}$ denote the averaging by $|\mathbf{r} - \mathbf{r}_p| \lesssim R_c$, and

$$\begin{aligned} \delta \mathbf{u}(\mathbf{r}_1, \mathbf{r}_2, t) = & [\mathbf{u}(\mathbf{r}_1, t) - \mathbf{u}(\mathbf{r}_1, t - T)] - \\ & - [\mathbf{u}(\mathbf{r}_2, t) - \mathbf{u}(\mathbf{r}_2, t - T)] \end{aligned} \quad (\text{S16})$$

Here the displacement $\mathbf{u}(\mathbf{r}, t)$ can consist of the ac near-elastic as well as the dc dissipative parts, both related to the ac and dc components of $\mathbf{V}(\mathbf{r}, t)$ by Eq. (S6).

In the hydrodynamic regime, the characteristic spacescale of the inhomogeneity of the flow, W , is much larger than R_c , therefore we have:

$$u_m(\mathbf{r}_1, t') - u_m(\mathbf{r}_2, t') \approx (x_{1n} - x_{2n}) \frac{\partial u_m(\mathbf{r}_1, t')}{\partial x_n}, \quad (\text{S17})$$

where the summation by n is supposed. Thus the expression $\delta \mathbf{u}(\mathbf{r}_1, \mathbf{r}_2, t)$ (S16), averaged by \mathbf{r}_1 and \mathbf{r}_2 , is expressed via the shift (the ‘‘mismatch’’) $\Delta_{mn}(\mathbf{r}, t)$ of the strain tensor $\varepsilon_{mn}(\mathbf{r}, t)$ in a cyclotron period. For the resulting $\hat{\Gamma}$ we obtain:

$$\hat{\Gamma}_{ijkl}[\mathbf{u}(\mathbf{r}', t')](\mathbf{r}, t) = \Gamma_{ijkl}(\Delta_{mn}(\mathbf{r}, t)), \quad (\text{S18})$$

$$\Delta_{mn}(\mathbf{r}, t) = \varepsilon_{mn}(\mathbf{r}, t) - \varepsilon_{mn}(\mathbf{r}, t - T).$$

Expansion of Γ_{ijkl} by Δ_{mn} up to the quadratic order is:

$$\Gamma_{ijkl}(\Delta_{mn}) = \Gamma_{ijkl}^{(0)} + \alpha_{ijkl}^{mnop} \Delta_{mn} \Delta_{op}, \quad (\text{S19})$$

where the tensors $\Gamma_{ijkl}^{(0)}$ and α_{ijkl}^{mnop} are determined by the parameters of the fluid and depend on temperature and magnetic field. The linear term $\alpha_{ijkl}^{mnop} \Delta_{mn}$ is absent in Eq. (S19) due to the symmetry of the relaxation processes relative to the inversion of the direction of flows.

From Eq. (S6) we obtain the expression for the mismatch of the strain tensor via the velocity gradient $V_{mn}(\mathbf{r}, t')$:

$$\Delta_{mn}(\mathbf{r}, t) \approx \int_{t-T}^t dt' V_{mn}(\mathbf{r}, t'). \quad (\text{S20})$$

Here, similarly to Eqs. (S8), the tensor V_{mn} can contain both the ac component corresponding to an almost elastic dynamics and the dc component corresponding to a dissipative viscous motion.

In this way, we formulated a closed system of equations, Eqs. (S7) and (S18)-(S20), describing the dynamics of the highly viscous 2D electron fluid with the memory effects in the interparticle scattering in a magnetic field. We remind that these equations provide only a simplest version of a phenomenological theory of such fluid.

According to Fig. S1, one should expect that the tensors $\Gamma_{ijkl}^{(0)}$ and α_{ijkl}^{mnop} are proportional to the probability

$$P = e^{-T/\tau_q}, \quad (\text{S21})$$

similar to probability (S2), to make a full cyclotron rotation without collisions with other quasiparticles and to some interparticle scattering rate, apparently, the rate of the relaxation of the shear stress $1/\tau_2$. Now the time τ_q in P is the departure time (that is, the quantum lifetime) relative to the interparticle collisions.

Within the described model of extended collisions [see Fig. S1 and Eqs. (S11)-(S20)], the relative value of the correction to the probability of an extended collision from the deviation of the trajectories $\mathbf{r}_{0,p}(t)$ from exact cyclotron circles is proportional to the squared ratio $|\delta(t)|/a_B$. The value

$$|\delta(t)| \sim \|\hat{\Delta}(\mathbf{r}, t)\| R_c \quad (\text{S22})$$

is the characteristic difference of the mismatches of the trajectories of quasiparticles near the point \mathbf{r} at the moment t and a_B is the Bohr radius, being the estimate for the size of the interparticle interaction potential. In this way, according to the definition of the tensors $\Gamma_{ijkl}^{(0)}$ and α_{ijkl}^{mnop} in Eq. (S19), we have:

$$\Gamma_{ijkl}^{(0)} = A_{ijkl} \frac{e^{-T/\tau_q}}{\tau_2}, \quad (\text{S23})$$

$$\alpha_{ijkl}^{mnop} = B_{ijkl}^{mnop} \left(\frac{R_c}{a_B} \right)^2 \frac{e^{-T/\tau_q}}{\tau_2},$$

where A_{ijkl} and B_{ijkl}^{mnop} are the numeric constants (apparently, of the order of unity) independent on the fluid parameters. We remind that for the case of the electron scattering on soft impurities, analogous formulas for the memory constants α and β in the tensor (S3) were derived in Ref. [22].

Formulas (S23) lead to a definite dependence of the retarded relaxation terms on the magnetic field (via T and R_c) and on the temperature T_e of the electron fluid via the times τ_2 and τ_q . The departure time τ_q is usually somewhat smaller than the stress relaxation time τ_2 , but they has similar temperature dependencies for 2D degenerate electrons at any strength of interparticle interaction [41, 42]. Up to the logarithmic factor $\ln(\varepsilon_F/T_e)$, being weakly dependent on the temperature T_e , both the rates $1/\tau_q$ and $1/\tau_2$ are the quadratic functions of T_e [41, 42]:

$$\frac{\hbar}{\tau_{q,2}} = C_{q,2}(T) \frac{T_e^2}{\varepsilon_F}. \quad (\text{S24})$$

Here ε_F is the Fermi energy of the electron fluid and $C_{q,2}(T_e)$ are the dimensionless coefficients, which are determined by the interparticle interaction parameter r_s , related to the electron density n_0 , and can weakly depend on temperature via the logarithm $\ln(\varepsilon_F/T_e)$.

2. Linear responses of highly viscous electron fluid on dc and ac electric fields

In order to study the photoresistance effect within the proposed model, first of all, we need to find the linear responses of the fluid on a dc and an ac electric fields \mathbf{E}_0 and $\mathbf{E}_1(t)$.

Both these fields can be written as $\mathbf{E}(t) = \mathbf{E}(\omega) e^{-i\omega t} + c.c.$ with $\omega = 0$ and $\omega \neq 0$. The linear response should be calculated by linearized equations (S7) applied to the ω harmonics of the hydrodynamic velocity $\mathbf{V}(\mathbf{r}, t) = \mathbf{V}(\mathbf{r}, \omega) e^{-i\omega t} + c.c.$, the density perturbation $\delta n(\mathbf{r}, t) = \delta n(\mathbf{r}, \omega) e^{-i\omega t} + c.c.$, and the shear stress tensor $\hat{\Pi}(\mathbf{r}, t) = \hat{\Pi}(\mathbf{r}, \omega) e^{-i\omega t} + c.c.$, corresponding to the harmonics of $\mathbf{E}(t)$.

First, we formulate the resulting equations for the amplitudes $\mathbf{V}(\mathbf{r}, \omega) \sim \hat{\Pi}(\mathbf{r}, \omega) \sim \mathbf{E}(\omega)$ at a general geometry of a flow.

A solution of the last of equations (S7) without the memory effect term $-\Gamma_{iklm}(\mathbf{r}, t)\Pi_{lm}(\mathbf{r}, t-T)$ leads to the following linear relation between the time harmonics of the momentum flux $\Pi_{ij} = \Pi_{ij}(\mathbf{r}, \omega)$ and of the gradients of the harmonics of the velocity $V_{ij}(\mathbf{r}, \omega) = \partial V_i / \partial x_j + \partial V_j / \partial x_i$ [38]:

$$\Pi_{ij} = m [\eta_{xx}(\omega) V_{ij} + \epsilon_{ikz} \eta_{xy}(\omega) V_{kj}], \quad (\text{S25})$$

where the ac viscosity coefficients $\eta_{xx} = \eta_{xx}(\omega)$ and $\eta_{xy} = \eta_{xy}(\omega)$ have the form [38]:

$$\left. \begin{array}{l} \eta_{xx} \\ \eta_{xy} \end{array} \right\} = \frac{(v_F^n)^2 \tau_2 / 4}{1 + (4\omega_c^2 - \omega^2) \tau_2^2 - 2i\omega \tau_2} \begin{cases} 1 - i\omega \tau_2 \\ 2\omega_c \tau_2 \end{cases}. \quad (\text{S26})$$

The second of equations (S7) with $\hat{\Pi}(\mathbf{r}, \omega)$ from Eq. (S25) is transformed into the Navier-Stokes equation for the harmonic of the velocity $\mathbf{V} = \mathbf{V}(\mathbf{r}, \omega)$:

$$-i\omega \mathbf{V} = \frac{e}{m} \mathbf{E}(\omega) + [\mathbf{V} \times \boldsymbol{\omega}_c] + \quad (\text{S27})$$

$$+ \eta_{xx}(\omega) \Delta_L \mathbf{V} + \eta_{xy}(\omega) \Delta_L \mathbf{V} \times \mathbf{e}_z,$$

where $\Delta_L = \partial^2 / \partial x^2 + \partial^2 / \partial y^2$ is the Laplace operator.

The role of the retarded relaxation term in the last of equations (S7) for the linear response is as follows. If we choose the main part $\hat{\Gamma}^{(0)}$ of the relaxation tensor $\hat{\Gamma}(\mathbf{r}, t)$ in the simplest form:

$$\Gamma_{ijkl}^{(0)} = \delta_{ik} \delta_{jl} \frac{1}{\tau_2'}, \quad (\text{S28})$$

we arrive to a redefinition of the relaxation rate $1/\tau_2$ which enters Eq. (S26) as compared with its value in the absence of the memory effects:

$$\frac{1}{\tau_2} \rightarrow \frac{1}{\tau_2} + \frac{e^{2\pi i \omega / \omega_c}}{\tau_2'}. \quad (\text{S29})$$

For the time τ_2' here we should use estimate (S23): $1/\tau_2' \sim e^{-T/\tau_q} / \tau_2$.

Further in this work we do not take into account redefinition (S29) of τ_2 by the two reasons. First, in view of estimate (S23), the second term in this formula seems to be much smaller than the first one on the factor e^{-T/τ_q} , which is substantially smaller than unity at $\omega_c \sim \omega \gg 1/\tau_2, 1/\tau_q$. Second, our analysis shows that redefinition (S29) leads only to some subtle distortion of the sinusoidal dependence of a factor in the resulting photoconductivity on the ratio ω/ω_c . For the current work, being a first proposal of the hydrodynamic mechanism of MIRO, such detail is not substantial.

We remind that the parameter v_F^n in Eq. (S26) for a strongly non-ideal electron Fermi liquid with large Landau parameters, $F_m \gg 1$, is much greater than the actual Fermi velocity v_F [23, 40].

Second, we use equations (S26) and (S27) to calculate the linear response of the electron fluid on the applied dc and the ac fields, \mathbf{E}_0 and $\mathbf{E}_1(t)$, in a Poiseuille-flow like geometry: a long straight sample with rough edges [see Fig. 1(a) in the main text]. We consider that the sample width W is much smaller than the characteristic plasmon wavelength l_p :

$$W \ll l_p, \quad l_p = s/\omega. \quad (\text{S30})$$

Here the estimate of l_p for a quantum well with a metallic gate is presented and s is the plasmon velocity in such structure which is usually much larger than v_F and v_F^n . In defectless samples of such widths the dc and ac linear responses are formed mainly by a dissipative viscous flow and by standing magnetosonic waves, respectively, whereas the plasmonic contribution to the ac flow component is suppressed to the extent of the small parameter $v_F^n/s \ll 1$ [23].

In such flow geometry, only the x component of the velocity $\mathbf{V}(y, t)$ and the xy component of the velocity gradient tensor $V_{ij}(y, t)$ are substantial [23]. For the ac flow component, the density perturbation $\delta n(y, t)$ and the y component of the velocity $V_{y,1}(y, t)$ are relatively small quantities being proportional to $(v_F^n/s)^2 \ll 1$ [23]. However, such δn determines the not small ac component $E_{y,1}^{int}(y, t)$ of the internal Hall field, which screens the y component of the radiation fields $E_{y,1}(t)$ [see Eqs. (S8)]. For the dc flow component, $V_{y,0} \equiv 0$ and the density perturbation $\delta n(y)$ determines the dc part of the Hall field $E_{y,0}^{int}(y)$. The x -component of equation (S27) for the hydrodynamic velocity $V_x(y) \equiv V(y)$ takes the form:

$$-i\omega V = \frac{e}{m} E_x(\omega) + \eta_{xx}(\omega) \frac{d^2 V}{dy^2}. \quad (\text{S31})$$

The both fields $E_{y,0}^{int}(y)$ and $E_{y,1}^{int}(y, t)$ are calculated from the y -components of equation (S27) [13].

The resulting response of the fluid in such sample on a dc electric field $\mathbf{E}_0^{ext} = E_0 \mathbf{e}_x$ is the dc Poiseuille flow with a parabolic profile. From Eq. (S31) at zero frequency,

$\omega = 0$, with the diffusive boundary conditions:

$$V|_{y=\pm W/2} = 0, \quad (\text{S32})$$

we obtain for the dc component V_0 of the velocity V [13]:

$$V_0(y) = \frac{eE_0}{2m\eta_{xx}} \left[\left(\frac{W}{2} \right)^2 - y^2 \right], \quad (\text{S33})$$

where the dc diagonal viscosity coefficient is:

$$\eta_{xx} = \eta_{xx}(0) = \frac{(v_F^\eta)^2 \tau_2 / 4}{1 + 4\omega_2 \tau_2^2}. \quad (\text{S34})$$

The corresponding averaged sample conductivity:

$$\sigma_0 = \frac{I_0}{E_0 W}, \quad I_0 = en_0 \int_{-W/2}^{W/2} dy V_0(y), \quad (\text{S35})$$

and the averaged resistivity $\varrho_0 = 1/\sigma_0$ strongly depend on a magnetic field via the viscosity coefficient η_{xx} [see Fig. 2(a) in the main text].

Next, we calculate the linear response of the fluid in the same long sample on the left and the right ac circularly polarized radiation fields:

$$\mathbf{E}^{ext}(t) = \mathbf{E}_1^\pm e^{-i\omega t} + c.c., \quad \mathbf{E}_1^\pm = \frac{E_1}{2} \begin{pmatrix} 1 \\ \pm i \end{pmatrix}. \quad (\text{S36})$$

As in was mentioned above, at condition (S30) the response is mainly formed by the transverse magnetosonic waves. According to Eq. (S31), the resulting velocity is almost independent on the sign “ \pm ” of the circular polarization of field (S36): $V_1^\pm(y, t) \approx V_1(y, t)$. From Eq. (S31) with the boundary condition (S32) we obtain $V_1(y, t) = V_1(y) e^{-i\omega t} + c.c.$, where:

$$V_1(y) = \frac{eE_1}{2m} \frac{i}{\omega} \left[1 - \frac{\cosh(\lambda y)}{\cosh(\lambda W/2)} \right], \quad (\text{S37})$$

and $\lambda = \lambda(\omega, \omega_c)$ is the eigenvalue corresponding to the transversal magnetosonic waves. It is seen from Eq. (S31) that:

$$\lambda = \sqrt{\frac{-i\omega}{\eta_{xx}(\omega)}}. \quad (\text{S38})$$

The reciprocal imaginary and real parts of this eigenvalue, $1/\text{Im}\lambda$ and $1/\text{Re}\lambda$, provide the wavelength and the decay length of the magnetosonic waves, respectively. Their dependencies on ω_c at a fixed frequency $\omega \gg 1/\tau_2$ are drawn in Fig. S2.

Far above from the viscoelastic resonance ($\omega - 2\omega_c \gg 1/\tau_2$) we obtain from Ref. (S38) the following estimates for the length of decay and the wavelength of magnetosonic waves:

$$\frac{1}{\text{Re}\lambda} \sim L_s = v_F^\eta \tau_2, \quad \frac{1}{\text{Im}\lambda} \sim l_s = \frac{v_F^\eta}{\omega}, \quad (\text{S39})$$

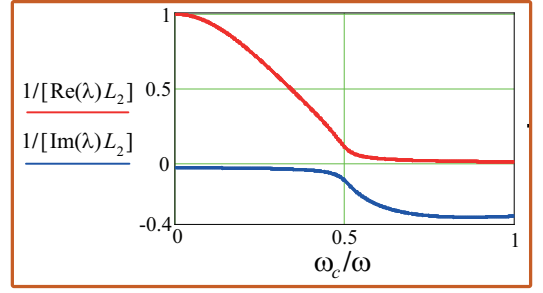


FIG. S2: Reciprocal real and imaginary parts of the eigenvalue λ , describing the decay length and the wavelength of the transverse magnetosonic waves, as the functions of a magnetic field at a high ac frequency, $\omega\tau_2 = 20$.

which lead to the relation $1/\text{Re}\lambda \gg 1/\text{Im}\lambda$. In this regime the solution $V_1(y, t) \sim e^{-i\omega t + \lambda y}$ is well-formed weakly decaying waves.

Far below the viscoelastic resonance ($2\omega_c - \omega \gg 1/\tau_2$), visa versa, we have:

$$\frac{1}{\text{Re}\lambda} \sim l_s, \quad \frac{1}{\text{Im}\lambda} \sim L_s, \quad (\text{S40})$$

thus $1/\text{Re}\lambda \ll 1/\text{Im}\lambda$. In this case the velocity profile $V_1(y, t) \sim e^{-i\omega t + \lambda y}$ is formed by exponentially decaying non-oscillating eigenmodes, and the imaginary part of λ is not substantial.

It follows from Eqs. (S37)-(S39) that above the resonance, $\omega > 2\omega_c$, the standing magnetosonic waves $V_1(y, t) \sim e^{-i\omega t + \lambda y}$ are formed. They are localized in the whole sample at the intermediate sample widths:

$$l_s \ll W \ll L_s, \quad (\text{S41})$$

and in the near-edge regions, $W/2 - |y| \lesssim L_s$, in the samples with the large widths (provided $L_s \ll l_p$):

$$L_s \ll W \ll l_p. \quad (\text{S42})$$

In the last case, the flow in the central part of the sample, $W/2 - |y| \gg L_s$, is a trivial response of a dissipativeless homogeneous electron media on the x -component of the ac field $E_{1,x}(t)$ [the first term in Eq. (S37)].

From Eq. (S40) it is seen that at the frequencies below the resonance, $\omega < 2\omega_c$, in the samples with the widths $W \gg l_s$ the ac response $V_1(y, t)$ is located in the narrower near-edge regions, $W/2 - |y| \lesssim l_s$ and have non-oscillation exponential profile.

It also follows from Eqs. (S37)-(S40) that in the narrowest samples,

$$W \ll l_2, \quad (\text{S43})$$

the velocity profile $V_1(y)$ is parabolic in both the cases $\omega > 2\omega_c$ and $\omega < 2\omega_c$, and its amplitude $V_1(0)$ decreases with the decrease of W as $\sim |\lambda|^2 W^2$.

Now we are able to calculate the shift (mismatch) of the xy component of strain tensor, $\Delta_{xy}(\mathbf{r}, t)$ in a cyclotron period, that enters the retardation relaxation term $-\Gamma_{ijkl}[\hat{\Delta}(\mathbf{r}, t)]\Pi_{kl}(\mathbf{r}, t - T)$ in the motion equation (S7) for the Poiseuille flow. In the presence of both the dc and ac fields \mathbf{E}_0 , $\mathbf{E}_1(t)$, as it takes place in the experiments of photoresistance, the shift $\Delta_{xy}(\mathbf{r}, t) \equiv \Delta(\mathbf{r}, t)$ in the linear approximation by E_0 and E_1 contains the two contributions:

$$\Delta(y, t) = \Delta_0(y) + \Delta_1(y, t), \quad (\text{S44})$$

from the dc dissipative and the ac almost elastic components of the linear response: $V_{lin}(y, t) = V_0(y) + V_1(y, t)$. Equations (S20), (S33), and (S37) yield:

$$\Delta_0(y) = \frac{2\pi}{\omega_c} \frac{dV_0}{dy} \quad (\text{S45})$$

and $\Delta_1(y, t) = \Delta_1(y) e^{-i\omega t} + c.c.$, where

$$\Delta_1(y) = \frac{i}{\omega} \left[1 - e^{2\pi i \omega / \omega_c} \right] \frac{dV_1}{dy}. \quad (\text{S46})$$

It is noteworthy that this formula contain the factor $e^{2\pi i \omega / \omega_c}$ being periodic by the reciprocal magnetic field.

3. Non-linear response of highly viscous fluid on dc and ac electric fields

In this section we calculate the nonlinear correction to the dc flow component $V_0(y)$ (S33) induced by the ac component $V_1(y, t)$ (S37) and the memory relaxation term in Eqs. (S7).

We continue to consider the flow in a long sample with the width W , which is much smaller than the characteristic plasmon wavelength l_p [Eq. (S30)]. Similarly as for the linear component, only the x component of the velocity \mathbf{V} and the xy components of the tensors V_{ij} and ε_{ij} present in the non-linear component [see Fig. 1(a) in the main text]. Equations (S7) take the simplified form:

$$\left\{ \begin{array}{l} \frac{\partial V}{\partial t} = \frac{e}{m} E^{ext}(t) - \frac{1}{m} \frac{\partial \Pi_{xy}}{\partial y} \\ \frac{\partial \Pi_{xx}}{\partial t} = 2\omega_c \Pi_{xy} - \frac{\Pi_{xx}}{\tau_2} - \Gamma(\Delta) \Pi_{xx}(y, t - T) \\ \frac{\partial \Pi_{xy}}{\partial t} = -2\omega_c \Pi_{xx} - \frac{\Pi_{xy}}{\tau_2} - \frac{m(v_F^\eta)^2}{4} \frac{\partial V}{\partial y} - \Gamma(\Delta) \Pi_{xy}(y, t - T) \end{array} \right. , \quad (\text{S47})$$

where $E^{ext}(t) = E_0 + E_{x,1}(t)$ and we used the simplest form of the retarded relaxation tensor $\Gamma_{ijkl} = \Gamma \delta_{ik} \delta_{jl}$,

similar to Eq. (S28). For the dependence of Γ on Δ , according to Eq. (S19), we write:

$$\Gamma(\Delta) = 1/\tau_2' - \alpha \Delta^2, \quad \alpha > 0. \quad (\text{S48})$$

The positiveness of α corresponds to the decrease of the probability for a particle “1” to scatter again on a particle “2” with the increase of the amplitudes of the velocity $V(y, t)$, of the strain $\varepsilon_{xy}(y, t)$, and, thus, of the trajectories mismatches $\delta_{1,2}(t)$ during a cyclotron period (see Fig. S1). Note that the same sign of the analogous parameters α and β in the tensor (S3) of the memory effect in the scattering of non-interacting electrons on defects was obtained in Ref. [22].

The mismatch $\Delta = \Delta(y, t)$ in Eqs. (S47) and (S48) is expressed via the integral of $\partial V(y, t')/\partial y$ by Eq. (S20).

The photoconductivity and the photoresistance at small ac powers are given by the correction to the dc current I_0 (S35), linear by the ac power $\mathcal{W} \sim E_1^2$. Thus, together with the linear responses $V_0 \sim E_0$ and $V_1 \sim E_1$, one needs to calculate the time-independent nonlinear component V_ω of the dc flow of the order of $\sim E_0 E_1^2$:

$$V(y, t) = V_0(y) + V_1(y, t) + V_\omega(y), \quad (\text{S49})$$

and the corresponding contribution $\hat{\Pi}_\omega \sim E_0 E_1^2$ to the momentum flux tensor:

$$\hat{\Pi}(y, t) = \hat{\Pi}_0(y) + \hat{\Pi}_1(y, t) + \hat{\Pi}_\omega(y). \quad (\text{S50})$$

Here $\hat{\Pi}_0$ and $\hat{\Pi}_1$ are the linear contributions in $\hat{\Pi}$, which are related to V_0 and V_1 by Eq. (S25).

The equations for $\hat{\Pi}_\omega$ and V_ω are derived by the substitution of the dc and the ac linear components, $\hat{\Pi}_0$, Δ_0 and $\hat{\Pi}_1$, Δ_1 , into the nonlinear parts of the retarded relaxation terms in Eqs. (S47) with $\Gamma(\Delta)$ (S48) and by the integration of the resulting equations for $\partial \mathbf{V}/\partial t$ and $\partial \hat{\Pi}/\partial t$ by one cyclotron period. After such procedure, we obtain:

$$\left\{ \begin{array}{l} \frac{\partial \Pi_{\omega,xy}}{\partial y} = 0 \\ \frac{\Pi_{\omega,xx}}{\tau_2} - 2\omega_c \Pi_{\omega,xy} = \\ \quad = \alpha \langle \Delta^2(y, t) \Pi_{xx}(y, t - T) \rangle_\omega \\ 2\omega_c \Pi_{\omega,xx} + \frac{\Pi_{\omega,xy}}{\tau_2} = -\frac{m(v_F^\eta)^2}{4} \frac{dV_\omega}{dy} + \\ \quad + \alpha \langle \Delta^2(y, t) \Pi_{xy}(y, t - T) \rangle_\omega \end{array} \right. \quad (\text{S51})$$

Here the angular brackets with the subscript “ ω ” denote the operation of taking the contribution of the order of $\sim E_0 E_1^2$, averaged by the last cyclotron period:

$$\langle f(t) \rangle_\omega = \frac{1}{T} \int_{t-T}^t dt' f_\omega(t'), \quad (\text{S52})$$

and $f_\omega(t) = f_{12}(t)E_0E_1^2$ denotes the term “12” in the decomposition of the function $f(t)$ in power series by the amplitudes of the dc and the ac fields: $f(t) = \sum_{m,n=1}^{\infty} f_{mn}(t)E_0^m E_1^n$.

From the last two equations in system (S51) we obtain the expression for the nonlinear part $\bar{\Pi}_\omega$ of the momentum flux tensor. In particular, for the xy component we have:

$$\begin{aligned} \Pi_{\omega,xy}(y) &= -m \eta_{xx} \frac{dV_\omega}{dy} + \\ &+ \frac{\alpha\tau_2}{1 + 4\omega_c^2\tau_2^2} \left[\langle \Delta^2(y,t) \Pi_{xy}(y,t-T) \rangle_\omega - \right. \\ &\left. - 2\omega_c\tau_2 \langle \Delta^2(y,t) \Pi_{xx}(y,t-T) \rangle_\omega \right]. \end{aligned} \quad (\text{S53})$$

Here the nonlinear terms in the brackets $\langle \dots \rangle_\omega$ (S52) contain the two contributions with the different combinations of the dc dissipative and the ac almost-elastic linear responses:

$$\begin{aligned} \langle \Delta^2(y,t) \Pi_{ij}(y,t-T) \rangle_\omega &= \\ &= \langle \Delta_1^2(y,t) \rangle \Pi_{0,ij}(y) + \\ &+ \langle \Delta_1(y,t) \Pi_{1,ij}(y,t-T) \rangle \Delta_0(y), \end{aligned} \quad (\text{S54})$$

where $ij = xx$ or $ij = xy$ and the angular brackets without a subscript denotes the operation of averaging over the last cyclotron period:

$$\langle g(t) \rangle = \frac{1}{T} \int_{t-T}^t dt' g(t'). \quad (\text{S55})$$

The linear components of the momentum flux tensor in Eq. (S54) have the form [see Eq. (S25)]:

$$\Pi_{0,(xx/xy)}(y) = -m \eta_{xy/xx} \frac{dV_0}{dy} \quad (\text{S56})$$

and

$$\Pi_{1,(xx/xy)}(y,t) = -m \eta_{xy/xx} \frac{dV_1}{dy} e^{-i\omega t} + c.c. \quad (\text{S57})$$

In view of Eq. (S46), the squared shift of the deformation Δ_1^2 in Eq. (S54), averaged by $t-T < t' < t$, is:

$$\langle \Delta_1^2(y,t) \rangle = \frac{4}{\omega^2} \sin^2 \left(\frac{\pi\omega}{\omega_c} \right) \left| \frac{dV_1}{dy} \right|^2. \quad (\text{S58})$$

Due to Eqs. (S46) and (S57), the expression under the angular brackets in the last term in Eq. (S54), averaged by $t-T < t' < t$, takes the form:

$$\begin{aligned} \langle \Delta_1(y,t) \Pi_{1,(xx/xy)}(y,t-T) \rangle &= \\ &= \frac{2}{\omega} \text{Re} \left[i \eta_{xy/xx}(\omega) (e^{2\pi i\omega/\omega_c} - 1) \right] \left| \frac{dV_1}{dy} \right|^2. \end{aligned} \quad (\text{S59})$$

Substitution of formulas (S53)-(S59) for $\Pi_{\omega,xy}$ into the first of equations (S51) leads to the final equation for the nonlinear part of the flow profile $V_\omega = V_\omega(y)$:

$$\frac{d^2 V_\omega}{dy^2} = G(y), \quad (\text{S60})$$

where $G(y)$ is given by formulas (S45), (S46), and (S53)-(S59). Equation (S60) should be solved with the diffusive boundary conditions on the component $V_\omega(y)$: $V_\omega|_{y=\pm W/2} = 0$. The result takes the form:

$$V_\omega(y) = \frac{e^3 E_0 E_1^2 \alpha u + 2 \text{Re } v}{m^3 (v_F^\eta)^2 \omega^4} J(y), \quad (\text{S61})$$

where $J(y)$ is the dimensionless factor determining the profile of the nonlinear flow component:

$$J(y) = \frac{|\lambda|^2}{|\cosh(\lambda W/2)|^2} \int_{|y|}^{W/2} d\tilde{y} \tilde{y} |\sinh(\lambda \tilde{y})|^2 \quad (\text{S62})$$

and the dimensionless values u and v contain the dependence on the frequencies ω and ω_c :

$$u = 4 \sin^2 \left(\frac{\pi\omega}{\omega_c} \right) (-1 + 4\omega_c^2\tau_2^2), \quad (\text{S63})$$

$$\begin{aligned} v &= \frac{2\pi\omega}{\omega_c} \left[\sin \left(\frac{2\pi\omega}{\omega_c} \right) - 2i \sin^2 \left(\frac{\pi\omega}{\omega_c} \right) \right] \times \\ &\times \frac{(-1 + i\omega\tau_2 + 4\omega_c^2\tau_2^2)(1 + 4\omega_c^2\tau_2^2)}{1 + (4\omega_c^2 - \omega^2)\tau_2^2 - 2i\omega\tau_2}. \end{aligned} \quad (\text{S64})$$

A direct calculation of the factor $J(y)$ (S62) yields:

$$\begin{aligned} J(y) &= \frac{\nu^2 + \mu^2}{8\nu^2 \mu^2 |\cosh[(\mu - i\nu)W/2]|^2} \times \\ &\times \left\{ \mu^2 [-\cos(\nu W) + \cos(2\nu y) - \right. \\ &- \nu W \sin(\nu W) + 2\nu y \sin(2\nu y)] + \\ &+ \nu^2 [-\cosh(\mu W) + \cosh(2\mu y) + \\ &+ \mu W \sinh(\mu W) - 2ty \sinh(2\mu y)] \left. \right\}. \end{aligned} \quad (\text{S65})$$

where $\mu = \text{Re } \lambda$ and $\nu = -\text{Im } \lambda$. It is seen from Fig. S2 that both the values μ and ν are positive at any ω and ω_c . In the limiting cases of the narrow and the wide samples, $W \ll \min(1/\mu, 1/\nu)$ and $W \gg \max(1/\mu, 1/\nu)$, we obtain from Eq. (S65):

$$J(y) = \frac{(\nu^2 + \mu^2)^2}{4} \left[\left(\frac{W}{2} \right)^4 - y^4 \right] \quad (\text{S66})$$

and

$$J(y) = \frac{W(\nu^2 + \mu^2)}{4\mu} \left[1 - e^{-2\mu(W/2 - |y|)} \right]. \quad (\text{S67})$$

In this way, in the very narrow samples the profile of the flow perturbation $V_\omega(y)$ is a fourth-order parabola, while in the very wide samples it is almost flat in the central region, $W/2 - |y| \gg 1/\mu$, and exponentially goes to zero in the near-edge regions, $W/2 - |y| \lesssim 1/\mu$. For the samples with the intermediate widths, $\min(1/\mu, 1/\nu) < W < \max(1/\mu, 1/\nu)$, the component $V_\omega(y)$ contains comparable decaying and oscillating parts [see Eq. (S65)].

The profiles $V_\omega(y)$ and $V_1(y)$ for the medium and the narrow samples are drawn in Fig. S3.

From the resulting expressions (S61)-(S65) and estimate (S23) for the coefficient in the memory term, $\alpha = B(R_c/a_B)^2 e^{-T/\tau_q}/\tau_2$, one can find the magnetooscillations of the velocity $V_\omega(y)$ at any y . Note that $R_c = v_F/\omega_c$ contains the actual Fermi velocity, unlike the viscosity coefficients containing the parameter $v_F^\eta \gg v_F$. At the strong magnetic fields and the high ac frequencies, $\omega_c \sim \omega \gg 1/\tau_2$, for the point $y = 0$ corresponding to the typical values of $V_\omega(y)$ (see Fig. S3), we have:

$$V_\omega(0) = \sin^2\left(\frac{\pi\omega}{\omega_c}\right) V_\omega^{max,1} + \sin\left(\frac{2\pi\omega}{\omega_c}\right) V_\omega^{max,2} \quad (S68)$$

where the amplitudes of these two oscillating contributions are:

$$V_\omega^{max,1} = 16 \frac{e^3 E_0 E_1^2 v_F^2 \tau_2}{m^3 (v_F^\eta)^2 a_B^2 \omega^4} e^{-T/\tau_q} J \quad (S69)$$

$$V_\omega^{max,2} = -\frac{4\pi\omega\omega_c}{\omega^2 - 4\omega_c^2} V_\omega^{max,1}, \quad (S70)$$

and the dimensionless factor $J \equiv J(0)$ is:

$$J = \frac{|\lambda|^2}{|\cosh(\lambda W/2)|^2} \int_0^{W/2} d\tilde{y} \tilde{y} |\sinh(\lambda\tilde{y})|^2. \quad (S71)$$

From Eq. (S65) we obtain that above the viscoelastic resonance, $\omega > 2\omega_c$, when $\mu \ll \nu$ (see Fig. S2), the factor J for different sample width is estimated as:

$$J \sim \begin{cases} \nu^2 W/\mu, & W \gg 1/\mu \\ \frac{\nu^2 W^2}{\cos^2(\nu W/2)}, & 1/\nu \ll W \ll 1/\mu \\ \nu^4 W^4, & W \ll 1/\nu \end{cases}. \quad (S72)$$

This formula for the intermediate sample widths, $1/\nu \ll W \ll 1/\mu$, is valid far from the magnetosonic resonances those occur at the coincidence of the sample width W with a half-integer number of the wavelengths of transversal magnetosound [23]:

$$\nu W = \pi + 2\pi l, \quad (S73)$$

where $l = 0, \pm 1, \pm 2, \dots$. In those points, the denominator in Eq. (S72) is zero. Therefore in the vicinities of ω and

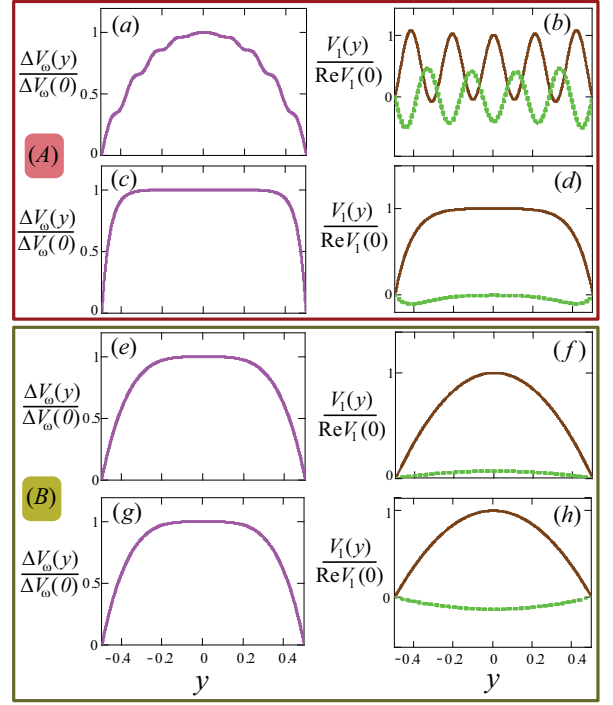


FIG. S3: Profiles of the flow components $V_\omega(y)$ [left panels] and $V_1(y)$ [right panels; brown lines refer to $\text{Re} V_1(y)$, green lines refer to $\text{Im} V_1(y)$]. All curves are plotted for the ac frequency $\omega\tau_2 = 40$. Panel (A) shows the results for a relatively wide sample, $W/L_s = 1$, in the magnetic fields $\omega_c\tau_2 = 0.34$ (a,b) and $\omega_c\tau_2 = 0.52$ (c,d). At $\omega_c\tau_2 = 0.34$ the system is above the viscoelastic resonance and the wavelength and the decay length of the magnetosonic waves are: $2\pi/(L_s \text{Im}\lambda) = 0.21$ and $1/(L_s \text{Re}\lambda) = 1.004$, whereas at $\omega_c\tau_2 = 0.52$ the system is below the resonance that correspond to the decay length $1/(L_s \text{Re}\lambda) = 0.031$. Panel (B) presents the results for a narrow sample, $W/L_s = 0.01$, at the magnetic fields $\omega_c\tau_2 = 0.34$ [(e,f); above the resonance; $\text{Im}\lambda$ and $\text{Re}\lambda$ are the same as in panels (a,b)] and to $\omega_c\tau_2 = 0.6$ [(g,h); below the resonance; $1/(L_s \text{Re}\lambda) = 0.038$].

ω_c corresponding to Eq. (S73) one should use the exact expression for the denominator: $|\cos[(\nu + i\mu)W/2]|^2$. Thus at $|\delta\omega_l| \ll 1$ and $\mu W \ll 1$ we have:

$$J \sim \frac{(\nu W)^2}{\Delta\omega_l^2 + (\mu W/2)^2}, \quad (S74)$$

where $\Delta\omega_l = \nu W/2 - (\pi/2 + \pi l)$.

Below the viscoelastic resonance, $\omega < 2\omega_c$, when $\mu \gg \nu$ (see Fig. S2), one obtains from Eq. (S65):

$$J \sim \begin{cases} \mu W, & W \gg 1/\mu \\ \mu^4 W^4, & W \ll 1/\mu \end{cases}. \quad (S75)$$

From Eqs. (S39), (S40), (S71)-(S75) we estimated the amplitudes $V_\omega^{max,1/2}$ (S69), (S70) in an exact form in the different regimes: above the viscoelastic resonance ($\omega > 2\omega_c$) for the wide [$W \gg 1/\mu(\omega_c)$], the medium

$[1/\nu(\omega_c) \ll W \ll 1/\mu(\omega_c)]$, and the narrow $[W \ll 1/\nu(\omega_c)]$ samples as well as below the viscoelastic resonance ($\omega < 2\omega_c$) for the wide $[W \gg 1/\mu(\omega_c)]$ and the narrow $[W \ll 1/\mu(\omega_c)]$ samples. We do not show all resulting formulas for $V_\omega^{max,1/2}$ in all these cases because of their cumbersomeness. We present only the result for the most interesting regime: above the viscoelastic resonance, $\omega > 2\omega_c \gg 1/\tau_2$, and for the medium sample width, $1/\nu \ll W \ll 1/\mu$, when the magnetooscillations acquire irregular shape [see Fig. 2(b) in the main text and Fig. S4(C)]. Far from the magnetosonic resonances (S73) the velocity amplitudes (S69) and (S70) in this regimes take the form:

$$V_\omega^{max,1} = (\omega^2 - 4\omega_c^2) V_\omega^0, \quad (\text{S76})$$

$$V_\omega^{max,2} = -4\pi\omega\omega_c V_\omega^0, \quad (\text{S77})$$

where

$$V_\omega^0 = C \frac{e^3 E_0 E_1^2 v_F^2}{m^3 (v_F^\eta)^4 a_B^2} \frac{W^2 \tau_2}{\omega^4} e^{-T/\tau_q} \quad (\text{S78})$$

and $C \sim 1/\cos^2(\nu W/2)$.

Now we can find the dependencies of the radiation-induced correction $\Delta\sigma_\omega$ to the dc conductivity, $\sigma = \sigma_0 + \Delta\sigma_\omega$, on temperature, the ac frequency, and magnetic field. The value $\Delta\sigma_\omega$ is defined as:

$$\Delta\sigma_\omega = \frac{I_\omega}{E_0 W}, \quad I_\omega = en_0 \int_{-W/2}^{W/2} dy V_\omega(y). \quad (\text{S79})$$

Equations (S76)-(S78) yield for the photoconductivity $\Delta\sigma_\omega$ in the described above most interesting case when the standing magnetosonic waves are well-formed:

$$\Delta\sigma_\omega = (U + V) \Delta\sigma_\omega^{max}, \quad (\text{S80})$$

where the factors $U = U(\omega/\omega_c)$ and $V = V(\omega/\omega_c)$ are:

$$U = \left[1 - \left(\frac{2\omega_c}{\omega} \right)^2 \right] \sin^2 \left(\frac{\pi\omega}{\omega_c} \right), \quad (\text{S81})$$

$$V = -\frac{4\pi\omega_c}{\omega} \sin \left(\frac{2\pi\omega}{\omega_c} \right)$$

and the amplitude $\Delta\sigma_\omega^{max} = \Delta\sigma_\omega^{max}(\omega, \omega_c\tau_q)$ is:

$$\Delta\sigma_\omega^{max} \sim \frac{e^4 E_1^2 n_0 v_F^2}{m^3 (v_F^\eta)^4 a_B^2} \frac{W^2 \tau_2}{\omega^2} e^{-2\pi/(\omega_c\tau_q)}. \quad (\text{S82})$$

Here the relaxation times $\tau_q = \tau_q(T_e)$ and $\tau_2 = \tau_2(T_e)$ are given by Eqs. (S24). It follows from this result that the oscillation of photoconductivity are suppressed with the increase of the temperature T_e and the ac frequency ω . It is seen from Eq. (S74) that in the vicinities of the magnetosonic resonances (S73) the value $\Delta\sigma_\omega^{max}$ increases as compared with Ref. (S82) in the large factor $\nu^2/\mu^2 \gg 1$.

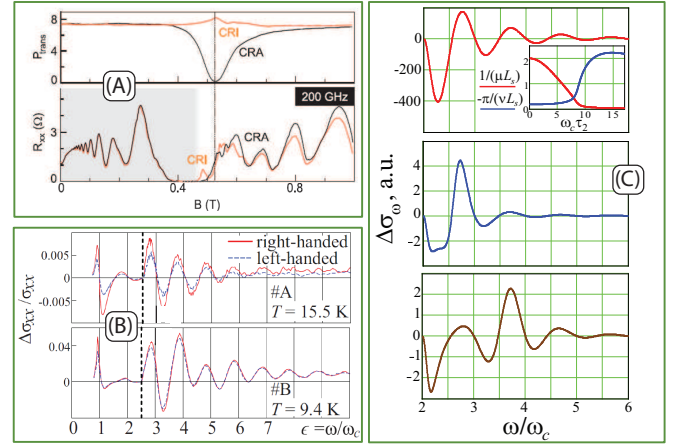


FIG. S4: (A) Experimental data on the cyclotron resonance in absorption (upper subpanel) and MIRO (lower subpanel) in an ultra-high quality GaAs quantum well with the experimental value of mobility $\mu = 18 \cdot 10^6$ cm²/V·s. Red and black curves refer to the inactive and the active circular polarizations of radiation. The figure is taken from Ref. [15]. (B) Experimental data on oscillating photoconductivity, analogous to MIRO, for two GaAs quantum wells: with a moderate experimental mobility (sample #A with $\mu = 0.82 \cdot 10^6$ cm²/V·s, upper subpanel) and with a relatively high mobility (sample #B with $\mu = 1.8 \cdot 10^6$ cm²/V·s, lower subpanel). The ac frequency is 0.69 THz. Red and blue curves refers to the right and the left circular polarizations. The figure is taken from Ref. [16]. (C) Results of calculations of the photoconductivity for a Poiseuille flow for the parameters $\omega\tau_2 = 17$, $\tau_q/\tau_2 = 0.7$, and different sample width: $W/L_s = 5.5, 0.85, 0.66$ for the upper, center, and lower subpanels, respectively. Inset: the dependencies of the length of decay ($1/\mu$) and one half of the wavelength ($-\pi/\nu$) of the transverse magnetosonic waves on $\omega_c\tau_2$ at $\omega\tau_2 = 17$ in the diapason $0 < \omega_c\tau_2 < \omega\tau_2$.

4. Comparison with experiment and discussion

Our theory predicts the irregular shape of the magnetooscillations of photoconductivity $\Delta\sigma_\omega$ at the intermediate sample widths (or, equivalently, the size of a flow) and the independence of $\Delta\sigma_\omega$ of the sign of the circular polarization of radiation. In Fig. S4 we compare these predictions with the experimental data. We cite the results of experiments [15, 16] on MIRO in high-quality GaAs quantum wells (panels A and B) and plot the theoretical curves (panel C) for Poiseuille flows with the parameters corresponding to the absence or to the occurrence of smeared magnetometric resonances at some ω/ω_c .

It is seen from Figs. 4S(A,B) that for the structure with the lower mobility (sample #A in panel B) there is some dependence of the MIRO-like photoconductivity on the polarization sign of radiation, whereas this dependence is almost absent for MIRO and for the MIRO-like photoconductivity in the ultra-high and the moderately high mobility samples (panel A and sample #B in panel B). It is also seen that for the lower mobility sample the shape

of oscillation is regular (sinusoidal with a slow damping with the increase of $1/B$), whereas for the two higher mobility samples the shapes are irregular: the amplitudes of some oscillations are too large or too small, but the other oscillations are sinusoidal with a slow damping with $1/B$. Apparently, the last fact, together with not very large absolute values of the amplitudes of the oscillations, evidence that the irregular shape of magnetooscillation appears already in the linear regime by radiation power.

As it was discussed in Section 2, the dependencies of $\Delta\sigma_\omega$ and $\Delta\rho_\omega$ on the polarization sign are absent in our theory, as we consider the relatively narrow samples, $W \ll l_p$ (S30), for which the viscoelastic contribution dominates in the ac flow component and thus $\mathbf{V}_1 \parallel \mathbf{e}_x$. Note that in the GaAs high-mobility quantum wells the macroscopic oval defects are often present [53], those can shape the flow and lead to the decrease of the actual width W of the flow from the sample width up to the mean distance between the oval defects $W_{eff} < W$ [13]. The dependence on the polarization sign can appear at sufficiently large sample, $W \gtrsim l_p$, owing to the formation of a substantial plasmonic component in V_1 or at a sufficiently large strength of disorder when the main contribution to photoconductivity is related to the scattering of quasiparticles on disorder (see comments [33, 34] and discussion in Ref. [30]).

Figure 4S(C) shows that the magnetooscillations of photoresistance within our theory at $\epsilon = \omega/\omega_c > 2$ are regular (sinusoidal with damping) in relatively wide samples, $W \gg l_s$, $W \gtrsim L_s$, and become irregular (some oscillations have peculiar values of amplitudes) in the narrower samples whose widths are comparable with the transversal sound wavelength l_s : $W \sim l_s$, $W \ll L_s$. These irregularities are the manifestations of magnetosonic resonances (S74), those are very smeared for the curves shown in panel C because of not very large value of $\omega\tau_2$. At larger values of $\omega\tau_2$ the irregularities become sharper [see Fig. 2(b) in the main text].

Below we will also consider the effects from particular violations of the maximal conditions of the applicability of the constructed purely hydrodynamic model: the absence of bulk disorder and the very large strength of the interparticle interaction.

First, as to the condition about the disorder, we will obtain below the estimates for sample and flow parameters at which the hydrodynamic contribution to the non-linear flow component can persist, despite of the substantial effect on the dc flow from the scattering of quasiparticles on bulk disorder. We will also present the resulting photoresistance and compare it with the experimental data on temperature and ac frequency dependencies of MIRO.

At high magnetic fields, $\omega_c\tau_2 \gg 1$, the magnitude of a purely hydrodynamic flow unlimitedly increases as ω_c^2 [see Eqs. (S33) and (S34)], thus the purely hydrodynamic

dc averaged resistance:

$$\rho_0 = \frac{E_0 W}{I_0}, \quad I_0 = en_0 \int_{-W/2}^{W/2} dy V_0(y), \quad (\text{S83})$$

strongly decreases with the increase of ω_c and W :

$$\rho_0 \propto \frac{1}{W^2 \omega_c^2}. \quad (\text{S84})$$

Such divergence is ‘‘healed’’ by the formation of an Ohmic flow in central region of the sample where the scattering of quasiparticles on disorder becomes to dominate and limits the magnitude of the current [13, 42]. Herewith the scattering of electron-like quasiparticles on phonons at sufficiently high temperatures can provide an additional contribution to the relaxation of a flow in the bulk.

The Ohmic contribution in the dc current I_0 dominates if the sample width is much larger than the Gurzhi length $l_G = l_G(\omega_c)$:

$$W \gg l_G, \quad l_G = \sqrt{\eta_{xx} \tau_{tr}}, \quad (\text{S85})$$

where $\tau_{tr} = \tau_{tr}(T_{ph})$ is the total momentum relaxation time due to the scattering of quasiparticles on bulk disorder and acoustic phonons. In this case, the Ohmic part of the flow is located in the central sample region:

$$y : W/2 - |y| \gg l_G. \quad (\text{S86})$$

The resulting hydrodynamic-Ohmic magnetoresistance is [see Fig. 2(a) in the main text]:

$$\rho_0 \sim \frac{\eta_{xx}}{W^2} + \frac{1}{\tau_{tr}}. \quad (\text{S87})$$

Note that the predicted hydrodynamic magnetooscillation of photoconductivity takes place at the high ac frequencies, $\omega\tau_2 \gg 1$ and in the following diapason of magnetic fields: $1/\tau_2 \ll \omega_c \sim \omega/2$.

At $\omega_c \sim \omega \gg 1/\tau_2$ the inequality (S85) can be consistent with inequality (S30), which ensures the dominance of the viscoelastic part in the ac component, if:

$$s \gg v_F^\eta \sqrt{\frac{\tau_{tr}}{\tau_2}}. \quad (\text{S88})$$

We remind that the plasmon velocity s in gated structures is usually far greater than v_F , whereas the parameter v_F^η is estimated as $v_F \sqrt{1 + F_2}$ [40], and the Landau parameter F_2 seems to be not far greater than unity at typical minimal densities $n_0 \sim 10^{11} \text{ cm}^{-2}$, when the interaction parameter is $r_s \sim 2$. Provided Eq. (S88) is fulfilled, for the frequencies $\omega \sim \omega_c$ in the interval:

$$\frac{v_F^\eta \sqrt{\tau_{tr}}}{W \sqrt{\tau_2}} \ll \omega \ll \frac{s}{W}, \quad (\text{S89})$$

the dc current component I_0 is predominantly due to the Ohmic flow $V_0(y) \approx \text{const}$ in the central (bulk) region (S86), whereas the ac flow component is still formed

mainly by the magnetosonic waves in the whole sample. Thus both the dc and ac flow components $V_0(y)$ and $V_1(y, t)$ in the near-edge regions:

$$y : W/2 - |y| \lesssim l_G, \quad (\text{S90})$$

are controlled by the viscosity and by the viscoelasticity effects, respectively.

In order to estimate the hydrodynamic photoconductivity $\Delta\sigma_\omega$ originating from these near-edge regions (S90), we can use the derived above formulas for $\Delta\sigma_\omega$ of a Poiseuille flow, changing in them the sample width, W or W_{eff} , on the characteristic width of the near-edge regions, l_G (S85). Herewith we assume that the contribution to photoconductivity from the bulk region (S86), which is controlled by the type and strength of disorder, can be neglected. Our estimations based on Eqs. (S82) and (S85) for $\Delta\sigma_\omega|_{W=l_G}$ and on the formulas from Refs. [30] and [22] for the different bulk contribution in $\Delta\sigma_\omega$ show that this assumption can be realistic.

In this way, when the Ohmic contribution in the dc conductivity σ_0 and the hydrodynamic contribution $\Delta\sigma_\omega$ of the near edge-layers (S90) in the nonlinear photoconductivity dominate, the averaged photoresistivity in the linear by ac power regime, $\Delta\rho_\omega \sim E_1^2$, takes the form:

$$\Delta\rho_\omega = -\Delta\sigma_\omega/\sigma_0^2, \quad (\text{S91})$$

where $\Delta\sigma_\omega$ is calculated by Eqs. (S82) and (S85) and the averaged Ohmic conductivity σ_0 of long samples is given by the usual Drude formula:

$$\sigma_0 = e^2 n_0 \tau_{tr} / m. \quad (\text{S92})$$

It is noteworthy that the last value has no dependence on magnetic field, the electron temperature, and the sample width.

As a result, we can estimate the dependence of the photoresistivity on magnetic field, ac frequency, and the electron and the phonon temperatures. For example, for the interval of the magnetic fields corresponding to the inequality $1/\nu \ll l_G(\omega_c) \ll 1/\mu$ and, thus, to the applicability of Eq. (S82), we obtain from equations (S80)-(S82), (S85), (S91), and (S92):

$$\Delta\rho_\omega = \sin^2\left(\frac{\pi\omega}{\omega_c}\right) \Delta\rho_\omega^{max,1} + \sin\left(\frac{2\pi\omega}{\omega_c}\right) \Delta\rho_\omega^{max,2}, \quad (\text{S93})$$

where

$$\Delta\rho_\omega^{max,1} = -\frac{A}{\omega^2 \omega_c^2} \left(1 - \frac{4\omega_c^2}{\omega^2}\right) e^{-B T_e^2 / \omega_c}, \quad (\text{S94})$$

and

$$\Delta\rho_\omega^{max,2} = \frac{4\pi A}{\omega^3 \omega_c} e^{-B T_e^2 / \omega_c}. \quad (\text{S95})$$

Here the values A and B are independent of ω , ω_c , T_e and are easily calculated from Eqs. (S82), (S85), and (S92). It

is seen from Eqs. (S94) and (S95) that at $1 < \omega/\omega_c < 4\pi$ the first amplitude, $\Delta\rho_\omega^{max,1}$, is numerically smaller than the second one, $\Delta\rho_\omega^{max,2}$.

The temperature and magnetic field dependencies of the amplitude of MIRO observed in Ref. [46] for a typical high-mobility GaAs quantum very well correspond to Eq. (S95), including the absence of a temperature dependence in the pre-exponent A . The formula used in Ref. [46] for fitting of the MIRO amplitude was just the same as Eq. (S95). A substantial temperature dependence of the pre-exponent amplitude of photoresistance oscillations was reported in Refs. [50, 51]. However, experiment [51] was performed for the GaAs structures with double quantum wells and in Ref. [50] a sufficiently different formulas for fitting of MIRO, as compared with the ones in Ref. [46], were used.

In this way, we think that the results on the temperature dependence of MIRO experimentally obtained in Ref. [46] are more relevant to the current discussion.

With the increase of ω , the shape of the modulated oscillations of $\Delta\rho_\omega$ as th function of the ratio ω/ω_c is retained in our theory [see Eqs. (S93)-(S95)]. The pre-exponent factor in the greater contribution $\Delta\rho_\omega^{max,2}$ (S95) at a fixed ratio ω/ω_c is rapidly suppressed with ω as $\sim 1/\omega^4$:

$$\frac{\Delta\rho_\omega^{max,2}}{(\omega/\omega_c) e^{-B T_e^2 / \omega_c}} = \frac{4\pi A}{\omega^4}. \quad (\text{S96})$$

Beside this, the destructive effect from inhomogeneities of the sample edges and from macroscopic defects inside the sample on the formation of the standing waves in the ac component begins to play a larger role with the increase of ω , as the wavelength $l_s = v_F^2/\omega$ decreases with ω . So a suppression and a smearing of the magnetosonic flow component and of its contribution to magnetooscillations of $\Delta\rho_\omega$ are expected with the increase of ω .

These predictions are in agreement with the measurements of MIRO in a high-mobility GaAs quantum well at the different frequencies ω in Ref. [50].

Second, let us discuss the role of disorder in the relatively narrow samples ($W \lesssim l_G$, $W \ll l_p$) in the limit of lowest temperatures T_e when any interparticle scattering is switched off.

At $T_e \lesssim 1$ K, MIRO as well as the giant negative magnetoresistance retain their characteristic features in experiments on GaAs quantum wells, while the scattering times τ_q and τ_2 obtained from fitting of experimental data attain some nonzero residual values [13, 14, 30, 42, 46] (see Fig. 3 in the main text). According to the discussions in Refs. [13, 14, 42], we hypothesize that in this limit of T_e the electron transport is still hydrodynamic-like, being described by the equations similar to equations (S7). Herewith it is unusual that the relaxation of the momentum flux density $\hat{\Pi}$, including the retarded relaxation, in this regime is determined by the scattering

of quasiparticles on bulk disorder. For the realization of such hydrodynamic-like regime one needs the shear stress relaxation time on disorder, $\tau_{imp,2}$, to be much shorter than the momentum relaxation time on the same disorder, $\tau_{imp,tr}$:

$$\tau_{imp,2} \ll \tau_{imp,tr}. \quad (\text{S97})$$

From the analysis of experimental data on the giant negative magnetoresistance it was concluded in Refs. [13, 14, 42] that this inequality actually is often realized in high-mobility GaAs quantum wells.

In this hydrodynamic-like regime of transport in the electron fluid, the same dependence of the viscosity $\eta_{xx}(\omega)$ on the frequencies ω and ω_c as well as the possibility of the excitation of shear stress transverse waves do retain. However the memory effects in the scattering of quasiparticles on disorder, similar in some aspects to the ones studied in Refs. [21, 22] will now determine the retarded relaxation of $\hat{\Pi}$ and the nonlinear components of the flow, instead of the memory effect in the interparticle scattering.

The giant negative magnetoresistance and the irregular shape of MRO are often observed in the same highest mobility samples up to the lowest temperatures [24, 25, 30]. This fact apparently point out on the realization of this hydrodynamic-like transport regime.

Third, let us discuss the violation of the condition about a very large strength of the interparticle interaction, leading to the possibility of using the the simple viscoelastic equations (S7) of a highly viscous fluid.

It is known that the shear stress transversal sound can be excited in an electron fluid not only at the very low densities n_0 corresponding to $r_s \gg 1$ and to large Landau parameters (the case of a highly viscous fluid):

$$F_m \gg 1, \quad (\text{S98})$$

but also at moderate densities, when $r_s \sim 1$ and $F_m \sim 1$ (the case of a moderately viscous fluid) [52, 54]. In the latter case, a high-frequency flow of the fluid is described not by the hydrodynamic variables n , \mathbf{V} , and $\hat{\Pi}$, but by the distribution function $f(\mathbf{r}, t, \mathbf{v})$ for the Fermi-liquid quasiparticles, which can consist of many comparable angular harmonics by the quasiparticle velocity \mathbf{v} . We remind that the hydrodynamic description by the variables

n , \mathbf{V} , and $\hat{\Pi}$ implies the predomination of only the zero, the first, and the second harmonics by \mathbf{v} in f .

It follows from a solution of the kinetic equation for f that the shear stress transverse waves are formed when the Landau parameters F_m are greater than some critical values $F_{m,c} \sim 1$ [52, 54]:

$$F_m > F_{m,c}, \quad (\text{S99})$$

those nontrivially depend on magnetic field. The memory effect in interparticle collisions described in Section 1 seems to persist at any r_s , provided the shape of a flow is non-homogeneous by \mathbf{r} and a substantial role is played by of the shear stress perturbations $\hat{\Pi}(\mathbf{r}, t)$. This memory effect and the excitation of the transversal waves can lead to temperature-dependent magnetooscillations of photoconductivity of the similar type, as in the case of a highly viscous fluid ($F_m \gg 1$), including the appearance of the irregular shape at certain W .

At the Landau parameters smaller than the critical values:

$$F_m < F_{m,c}, \quad (\text{S100})$$

the transverse shear stress waves cannot be excited, but the memory effect in the interparticle scattering is to persist, according to the essence of the mechanism illustrated by Fig. 1S. Thus the magnetooscillations of $\Delta_{\varrho\omega}$ within the hydrodynamic model also is to appear at condition (S100), but they can have only the sinusoidal shape due to the absence of the shear stress waves.

Finally, we should say that in sufficiently wide samples (for which, at least, the inequalities $W \gg l_p$, $W \gg l_G$ take place) MRO is to be predominantly due to the purely disorder bulk mechanisms, based on the consideration the quantum or the classical dynamics of independent 2D electrons in the presence of disorder, a magnetic field, and electric fields. These mechanisms were extensively studied to date [17–22, 30, 36]. However, as far as we know, that is an open question up to now, whether the irregular shape of magnetooscillations of photoresistivity (in the linear by radiation power limit) and its independence of the sign of the circular polarization of radiation can be deduced within some relevant disorder or disorder-free mechanism [33, 34].